Reply to Comments by Referee #1

We thank the referee for constructive and helpful comments to improve our manuscript. We copy the comments in italic and red. In the responses, we also indicate the changes made in the manuscript (in blue font).

Overarching suggestions

- In the intro, you explain that some of the uncertainty in greenhouse gas budgets could be due to different inverse modeling methodology. However, you use one flavor of Bayesian inverse modeling in the paper (albeit with different atmospheric models and prior estimates). I think you could strengthen the intro by framing this discussion around uncertainties in transport and uncertainties due to the prior – topics that you actually explore in depth in the paper.

What we present in this paper is what we can see in the atmospheric CH_4 observations at our new Canadian Arctic measurement sites and how we can detect the regional CH_4 emissions with these new measurements given uncertainties in the inversion modelling framework used in this study. We have modified the introduction to state our objectives in this study more specifically. Detailed changes are explained in the following, as we answer to the specific comments.

- I would be careful with the references throughout the text. In some cases, the references feel incomplete (particularly in the introduction), or you cite a reference that either did not focus primarily on that particular topic or was not the first to develop the concept.

As we revised the manuscript, we replaced some references with more adequate ones and also added references. For example, we now refer methane emissions from permafrost to McGuire et al. (2009); Schuur et al.(2015); Thornton et al. (2016), instead of the IPCC report, Ciais et al (2013). Other changes are shown in our responses to the specific comments.

- Most of the text in the results and discussion is dedicated to discussing more technical or methodological issues related to atmospheric transport, the inverse modeling setup, etc. I think the most interesting scientific conclusions of this paper are buried in Sect.4.6.3 at the end of the results and discussion section. I would consider de-emphasizing some of the more methodological elements of the discussion and move the bigger science questions to a more prominent place. For example, you could pose the most important science questions at the end of the intro; that would give the reader an idea of what to expect. You could also move Sect. 4.6.3 to the beginning of the results and discussion and lengthen that section. You could also move the more methodological components of the discussion to the end and shorten that text.

This section [Relationship of fluxes with climate anomalies] is scientifically interesting regarding climate change, in this paper. Before we get to the point, we first need to understand the robustness and uncertainties of the estimated regional CH_4 fluxes. That is why we have conducted inversion experiments using multiple atmospheric models, prior fluxes, and sub-region masks. Furthermore, this paper aims to present the new observational data of atmospheric CH_4 in the Canadian Arctic and the inferred regional fluxes utilising the new atmospheric observations. We anticipate

expanding this study to quantify a trend in CH_4 emissions as well as inter-annual variations in the Canadian Arctic with longer observational records in the future.

As suggested, we moved Section 4.6.3 forward (not to the beginning, but to Section 4.5) in Results and Discussions, after Section 4.4 (Comparison with previous estimates), where we mention the interanual variability of estimated fluxes, comparing with the results from CARVE. We lengthen this section (now Section 4.5) by adding the discussion on influence of prior fluxes. Note that the 3 different prior fluxes C1, C2 and C3 have been changed to the more descriptive names VIS, GEL and WetC following a specific comment. The previous Figure 12 is updated and shifted to Figure 11 to be consistent with the new modifications. These new names appear in the following:

4.5 Relationship of fluxes with climate anomalies

Inter-annual variations of estimated CH_4 fluxes are examined in relation to climate parameters here, specifically with surface air temperature and precipitation from NCEP reanalysis (Kalnay et al., 1996). First, monthly mean values at the sub-regions as well as the 4-year mean (2012-2015) for each month are calculated, then the monthly anomalies are computed from the monthly mean values and the 4-year mean of the corresponding month. The temperature and precipitation anomalies are aggregated to the respective regions, NT, YT and NU. On the regional level, climate anomalies in NT and NU are quite similar, though YT is less similar to NT and NU. YT is mainly covered by mountains with little wetland. Furthermore, NT has the largest wetland extent and most of the forest fire emissions in 2012-2015. Thus, we look into the correlation in monthly anomalies of CH_4 fluxes with summer climate anomalies in NT.

In Fig. 11, the inter-annual variability of wetland CH_4 fluxes exhibits a moderate positive correlation with the surface temperature anomaly ($r = 0.55$) and only weakly correlated with precipitation anomalies ($r = 0.11$). This indicates that the hotter summer weather condition stimulates the wetland CH_4 emission, and precipitation appears to have a less immediate or no direct impact on wetland conditions. In prior cases VIS and GEL, natural CH_4 fluxes (wetland and other fluxes except biomass burning CH_4 flux) are multi-year mean monthly fluxes. Therefore these prior fluxes have no year-to-year anomalies and no correlation with the meteorological anomalies. Only in WetC, the prior with wetland CH_4 fluxes from WetCHARTs ensemble mean exhibits inter-annual variations, the correlations with temperature and precipitation anomalies are $r = 0.26$ and $r = 0.90$ respectively. The posterior natural fluxes with WetC show slightly higher correlations ($r=0.55$ with temperature, $r=0.16$ with precipitation) than the mean correlation values. But overall there is no clear dependency of posterior correlations on the inherent climate anomaly correlations in the prior fluxes. This result indicates that the inter-annual variations in posterior wetland fluxes in this study are mainly determined by the observations, rather than by prior fluxes.

Inter-annual variations of estimated BB CH_4 fluxes show a negative correlation with precipitation ($r = -0.41$). Also throughout the fire season (June-September), all estimated BB fluxes negatively correlate with precipitation while the prior BB fluxes appear to have no consistent correlations. The inversion results support that dry condition would enhance the forest fire. The estimated BB fluxes show weakly negative correlation with surface temperature ($r = -$

0.23) on mid-summer average, but the monthly correlations are fluctuating from r = -0.40 to r = 0.47 over the fire season. Since the period is limited in this study (2012─2015), these statistical relationships are still not clear. Also, the relationship of CH_4 emissions with climate conditions could be complex and non-linear (with extreme fires events in some years). More data and analysis are required to characterise the dependence of CH_4 fluxes on climate in the Arctic.

Abstract:

- What provinces/territories or latitudes/longitudes do you define as the "Canadian Arctic"? That definition would help put the budget estimate in context.

We added latitude information (>60˚N, 60˚W─141˚W). Since the Canadian province and territories might not be familiar to some readers, it would be better to be introduced later, not in abstract.

- Abstract and throughout: The authors use the word "the" too often throughout the text. Some sentences would be smoother with fewer articles. For example, in line 9, "the regional CH4 flux" could be changed to "regional CH4 fluxes", and in line 10, "the recent observations" could be shortened to "recent observations." There are similar examples in most paragraphs of the manuscript.

We tried to omit "the' if it is not necessary in Abstract and throughout the manuscript to improve the readability.

Introduction:

- Pg. 2, lines 1-2: This sentence feels out of place. It does not summarize the content of the previous paragraph. Rather, it feels like the topic sentence of the paragraph starting in line 3.

We have moved the sentence to the next paragraph as a topic sentence, which is shown in the response to the next comment.

- Pg. 2, lines 3-24: I would restructure these paragraphs. In the first two paragraphs, you state several times that methane fluxes are uncertain and only provide detail in the third paragraph. I would condense these three paragraphs into one and provide specific numbers sooner in the text.

Following your comment, we have re-structured these paragraphs. Now the original third paragraph is the top and the first and second ones follow with modifications. Top sentence of the new first paragraph has been moved in from the immediate previous paragraph as answered to the previous comment:

The natural CH_4 flux estimates remain largely uncertain in higher northern. There have been many studies on CH_4 emission using bottom-up and top-down methods and Saunois et al. (2016) provide a thorough review of the different studies. In general, bottom-up flux estimates for the northern high latitudes from biogeochemical CH_4 models have large variations, and the mean estimate is much higher than top-down estimates from the inverse modelling (Saunois et al., 2016). For the Boreal North America region including Alaska and the Hudson Bay Lowlands (HBL, the second largest boreal wetland in the world), the bottom-up mean estimate is ~32 $TgCH_4\ yr^{-1}$, with a wide range

from 15 to 60 $TgCH_4$ yr^{-1}. On the other hand, the top-down estimate is ~12 $TgCH_4$ yr^{-1} with a narrower range from ~7 to 21 $TgCH_4$ yr^{-1}.

Bottom-up estimates from wetland methane models in WETCHIMP show large discrepancies in the spatial distribution of wetland CH_4 source, as well as its magnitude (Melton et al., 2013). In the higher latitudes, the limited ground-based information has hindered the mapping of wetland. Recently, remote sensing has been providing more information, but the high-latitude wetland extent still has large uncertainties (Olefeldt et al., 2016;Thornton et al., 2016). In addition to uncertainty in wetland extent, other factors affecting high-latitude wetland emissions in different models still remain. A recent inter-comparison of CH_4 wetland models (Poulter et al., 2017) in which all models used the same wetland extent, Surface Water Microwave Product Series (SWAMPS) (Schroeder et al, 2015) with Global Lakes and Wetland Database (GLWD) (Lehner and Döll, 2004) and same meteorological data (CRU-NCEP v4.0 reconstructed climate data) to drive their models showed a range in estimated CH_4 emission for North American Boreal/Arctic region which remains larger than that for other regions in the world. This large range of the CH_4 emissions for North American Boreal/Arctic region indicates the uncertainty in our current understanding of physical and biogeochemical processes that contribute to wetland CH_4 emissions.

- Pg. 2, line 25: What do you mean here by "the fluxes"? Are you referring to Arctic methane fluxes or greenhouse gas fluxes more broadly? The studies cited in this paragraph are not all methane studies.

This paragraph initially gave a general description of top-down inversion, not being specified for CH4 studies. Then "the fluxes" mean greenhouse gas fluxes broadly. To be more specific to methane inversion studies, we have modified the paragraph as restructuring along with the previous paragraphs (as we answer to the overarching suggestions). This paragraph has been modified, also as responding to the following two specific comments. The references are modified accordingly:

Top-down atmospheric inverse models have been developed to infer the CH_4 fluxes with observed atmospheric CH_4 mixing ratios as constraint. Global CH_4 inversion studies estimate global distribution of emissions and sinks from sites around the world and/or space (e.g., Bousquet et al., 2006, 2011; Bergamschi et al., 2013; Bruhweiler et al, 2014), but with limitted observational infromation in higher northern latitudes. Recently ground-based observation coverage in high northern latitudes has been improving, including towers and aircraft measuerments (e. g., Karion et al. 2016; Sasakawa et al 2010.; Chang et at., 2014). These observations have been used for CH_4 flux estimation in specific regions. For North America, previous atmospehric CH_4 studies were mainly foucued on Alaska (e.g., Miller et al., 2016; Hartery et al. 2018). Thompson et al., (2017) conducted CH_4 flux estiamte for entire region north of 50˚N, combining recent high-latitude surface observations. Estimated CH_4 emissions for the Canadian Arcitc show disctipancies among the inverse studies; the mean total CH_4 emission (2006-2010) is ~1.8 $TgCH_4$ by TM5-4DVAR (Bergamschi et al., 2013), 0.5 $TgCH_4$ by CarbonTracker-CH_4 (Bruhweiler et al, 2014), and 2.1 $TgCH_4$ by FLEXINVERT (Thompson et al., 2017). Differences including model transports, prior fluxes and observational datasets could affect the inversion results. The previous CH_4 inversion studies used only Alert in the Canadian Arctic,

the most northern site in the world. Several new sites in the Canadian Arctic (described in the next paragraph) might be helpful in constraining flux estimation.

- Pg. 2, line 26: 4Dvar, Kalman filter, and geostatistical studies are all Bayesian.

Yes, all of them are variations of Bayesian inversion. We do not intend to explore the details of different inversion schemes (as we used only one type of Bayesian scheme). As seen in our response to the previous comment, we have removed these detailed technical terms from the revised text.

- Pg. 2, lines 30-31: Can you provide references for this statement? Also, can you be more specific about how these differences have affected inverse modeling results in the past? What implications might those differences have for your study (i.e., for estimating Arctic methane)?

This statement listed some of the possible sources of uncertainties in inversion results. We agree it is too general to be informative and it has been deleted in the revision.

- Overall, the introduction includes a lot of broad, brush-stroke statements that sometimes lack specifics, and it is not always clear how these statements concretely relate to the present study. I think you could strengthen the introduction two ways: (1) provide more specific information to illustrate how uncertain or challenging these scientific questions are, and (2) Discuss why these uncertainties are particularly relevant to the present study or to understanding greenhouse gas fluxes from the Arctic.

As we answer in the next comment, we have modified the last two paragraphs to state more specifically what are challenging for estimating the Arctic greenhouse gas fluxes and our monitoring effort, as narrowing down to what we present in this study.

- Pg. 3, lines 7-12: I think it would be stronger to frame this study around specific scientific questions instead of framing the study around presenting and analyzing observations.

The last paragraph in the Introduction has been revised to focus more on the scientific questions as follows:

This is the first study to analyse the atmospheric CH_4 mixing ratios from the above new ECCC observation sites in the Canadian Arctic region. In this study, we address three key questions: (1) what can the new measurements see from local and regional sources? (2) what are the estimated CH_4 fluxes in the Canadian Arctic from inverse modelling using these new measurements? and (3) are there any relationship for the Canadian Arctic CH_4 fluxes with climate/environmental variations? This paper is structured as follows: In Section 2, the description of the measurement stations as well as the observational data analyses from daily to inter-annual time scales are given. Section 3 describes the inversion model framework, and Section 4 presents flux estimates and discusses the flux uncertainties and relationship to climate anomalies.

Measurements:

- Sect. 2.2: Some of this analysis might be a better fit for a results and discussion section than a methods section. Furthermore, it seems like the main conclusions of this paper center around the inverse modeling results. Hence, I think some of this detail could go into a supplement.

Since this is the first paper to analyse these new measurement data, we thought it is better to present the data analyses in the main text in a (mostly) self-contained section (for readers with more interest on the data characteristics than inversion results). We do show some analysis of the observed data with the model results in Section 4.2 [Signals in the observations (relative to the background)] where it is more appropriate.

Model description

- Sect. 3 title: Can you be more specific about which model you are referring to? The atmospheric transport model, the inverse model, or both?

The title is changed to 'Regional inversion model description'. We hope this is clearer as the atmospheric transport model (Section 3.1) is one component of the regional inverse model. We used different combinations of atmospheric transport model and atmospheric forcing data to help estimate the transport uncertainties in the inversion results.

- Pg. 7, line 13: I think the number of days required really depends upon the size of the domain and the geographic extent of the influence footprint.

Yes. Particle traveling time and size of domain of the interest are related. Bigger space/domain need more time (for the air particles to travel over). As seen in Figure 6, the 5-day footprint cover the Canadian Arctic, the domain of our interest and the location of the particles after 5 days are mostly outside the Canadian Arctic. Furthermore most synoptic-scale variations in the CH_4 mixing ratios at measurement sites are sufficiently explained by footprints within 2-5 days after particles are released.

- Pg. 7, line 24: Are you referring to a "model setting" or a "model setup"?

Since we describe the combinations of transport models and meteorological data that we used to obtain footprints, "model setup" would be more suitable than "model setting". We have replaced "model setting" with "model setup" here and other occurrences.

- Sect. 3.2: I think it would be helpful to have more descriptive flux model names than "C1", "C2", and "C3".

Each flux scenario consists of some different fluxes, but some common fluxes. The distinctive features are wetland CH_4 fluxes. To reflect the differences in Wetland CH_4 emission, we modified C1, C2 and C3 to VIS, GEL and WetC, respectively, as follows:

From C1 to VIS : VISIT CH4 wetland model,
From C2 to GEL : optimised fluxes by GELCA-CH_4 inversion
From C3 to WetC : WetCHARTs

- Sect. 3.2: Somewhere in the text, it could be useful to include a sentence that explains why you chose these three particular prior models.

We chose the first two cases of prior fluxes since the background atmospheric CH_4 fields is calculated by a global model NIES-TM with GELCA-CH_4 optimised fluxes. However, these fluxes are averaged to be cyclo-stationary (climatological). WetCHARTs provides inter-annually varying wetland CH_4 fluxes for the study period. CH_4 emissions of WetCHARTs are driven by environmental parameters, including satellite-based wetland extent.

The first paragraph of Section.3.2 has been revised as follows:

Three cases of prior emissions, VIS, GEL and WetC, were used as listed in Table 2. Since the global background atmospheric CH_4 field is calculated with GELCA-CH_4 inversion posterior fluxes, we chose the prior (VIS) and posterior (GEL) fluxes from the GELCA global inversion as two cases of prior fluxes in our regional inversion, respectively. Note that the continuous CH_4 mixing ratio data from the new Canadian Arctic sites were not used in the GELCA-CH_4 inversion. In this study, the mean wetland fluxes for the last 5 years of the GELCA global model were used, the prior forest fire CH_4 fluxes are detailed in Section 3.2.2. The third prior case (WetC) is the same as GEL, but with wetland CH_4 fluxes from WetCHARTs (a recent global wetland methane emission model ensemble for use in atmospheric chemical transport models). WetCHARTs provide inter-annually varying monthly wetland CH_4 fluxes for this study period. The details of prior fluxes are described in the following sections

- Pg. 10, lines 22-23: How did you decide on these values of sigma?

The sigma value for prior uncertainty, σ_{prior}=0.30, is from the uncertainty in the CH_4 emission used in Zhao et al. (2009). The prior model-mismatch, σ_e=0.33, is comparable to those used in previous regional inversion studies (e.g., Gerbig et al., 2013; Lin et al., 2004, Zhao et al., 2009), which considered different error components such as wind field, aggregation, and background CH_4 mixing ratio. We examined the sensitivity to these sigma values as explained in the next comment/response.

We have added the references for these sigma values in the revised manuscript.

- Pg. 10, line 24: What do you mean by "not strongly dependent"? Can you be more specific?

We have added more details to clarify lines 23-24:

We examined the inversion's sensitivity to these uncertainties by doubling their values. The posterior fluxes changed by less than 5% for all sub-regions (and the different sub-region masks). The results showed the optimised fluxes are not strongly dependent on these prescribed uncertainties.

- Eq. 2: Lin et al. 2004 did not derive this equation and are not the first ones to use it. Instead, I would cite a textbook by Rodgers, Tarantola, or Enting.

It is true that Lin et al. (2004) did not introduce this equation. We have added three textbooks as references for the Bayesian inversion approach at the beginning of the section: Tarantola (1987), Rodgers (2000) and Enting (2002). They collectively cover the basic concept and equations of Bayesian inversion and its applications of atmospheric greenhouse gases. We have removed the reference Lin et al.(2004).

- Pg. 11, line 7: The inverse model does not necessarily need to provide a perfect constraint on every region. Many modern inverse modeling studies estimate fluxes at model grid scale, even though the observations may not constrain each model grid box. If the observations do not provide a robust constraint at a particular location or time, the inverse modeling estimate will be guided by the prior estimate and the structure of the covariance matrix D_prior.

Yes, we do agree that it is possible to estimate fluxes for sub-regions not well constrained by observations, by using the additional information in the '*prior estimate and the structure of the covariance matrix D_prior*'. Given all the constraints, the estimated fluxes are still susceptible to (unaccounted for) errors such as model transport biases, non-Gaussian error distributions and other problems. In this study, we found that the weak flux region (Yukon) could not be robustly constrained (fluctuating from positive to negative fluxes). Hence, we explored different sub-region masks to test the robustness of the inversion results. We have clarified the statement with an addition as follows:

From:

The inversion results in the next section will show YT could not be reliably constrained as a separate sub-region.

To:

The inversion results in the next section will show YT could not be reliably constrained as a separate sub-region (model uncertainties made the estimated fluxes in YT fluctuate from positive to negative).

- Pg. 11, line 15: I think it would be useful to include one sentence explaining why you process the observations in this way.

We have added an explanation of the afternoon mean values:

First, the afternoon mean values are calculated by averaging the hourly data over 4 hours from 12:00 to 16:00 local time so that the observations we use in this study are more regionally representative assuming mid-day is in well-mixed planetary boundary layer. Second, the modelled background mixing ratio, which were described earlier, are subtracted from the afternoon means.

Results and discussion

- Sect. 4.1: Why do you think the footprints are different, and is there one you think is better or more robust than another?

The footprints are dependent on the meteorological fields, parametrized dispersions, etc. Thus the 'quality' or 'goodness' of the footprints could vary with time and place (as a function of the 'quality' of the meteorological forcings and dispersion model parametrizations, etc.). In the Canadian Arctic (particularly in summer), we found that for spatially distributed and slow varying fluxes like wetland CH4, the results are less sensitivity to the transport model difference, but fast varying and point like sources like biomass burning are quite sensitive to the model transport differences. Since it is difficult to separate the errors in transport and errors in emissions when comparing modelled and observed mixing ratios, we are mainly using the different transport models to provide an estimate of transport uncertainties in the inversion results.

- Sect. 4.2: I don't think this information is essential to the paper – if you're looking to trim the text at all. Presumably, this information should also be reflected in the posterior uncertainties of the inverse model.

We think this section could be informative for the general reader (not all working on inversion modelling). It provides an evaluation of the amount of the regional CH_4 signals in the model compared to the 'background' and an explanation on the relatively larger percentage error in the winter inversion results compared to the summer. Thus, Section 4.2 is potentially useful, we have decided to keep this section.

- Pg. 13, line 1: The word "significant" is often shorthand for "statistically significant." If you used a statistical test, I would clarify here with a p-value. If not, I would pick a different word than "significant" because that word may have specific meaning to many readers.

We have changed "significant" to "noticeable'.

- Sect. 4.6.1: This result seems unsurprising to me. The inverse model includes several observing stations and more observations than unknowns. As a result, the prior and the covariance matrices do not need to do much "work" in the inverse model. I suspect that one would get similar estimates using a linear regression to estimate the scaling factors.

It seems that our inversion results are not sensitivity to +/- 50% change in prior emission due to having sufficient regional signals compared to the background conditions. The summertime regional signals in atmospheric CH_4 is strong enough to infer regional fluxes, as we show in Section 4.2 [Signals in the observations (relative to background)]. In this section, we are trying to demonstrate that the results appear robust. We do agree that a 'linear regression estimate to the scaling factors' should work in this case. Given the strong observational constraints, the prior constraint term is likely not important.

Summary:

- The summary feels like an extended abstract. It also repeats the description of some of the methodology. You might consider changing this section to a conclusions section and instead contextualize the results, discuss the possible implications of these results, and potentially make recommendations for future monitoring efforts in the North American or Canadian Arctic.

We have changed the section title from summary to conclusions. We have also shortened the texts of the results, but stated more on a future direction and the implication of the study results as follows:

5 Conclusions

The Canadian Arctic region is one of the potential enhanced CH_4 source regions related to the ongoing global warming (AMAP, 2015), and earth system models differ in their prediction how the carbon loss there will be split up between CO_2 and CH_4 emissions. Even current bottom-up and top-down estimates of the CH_4 flux in the region vary widely. This study:

1) analysed the measurements of atmospheric CH4 mixing ratios that include 5 sites established in the Canadian Arctic by ECCC, to characterise the observed variations and examine the detectability of regional fluxes.

And,

2) estimated the regional fluxes for 4 years (2012─2015) with the continuous observational data of atmospheric CH_4, and also the relationship of the estimated fluxes with the climate anomalies.

The observational data analysis reveals large synoptic summertime signals in the atmospheric CH_4, indicating strong regional fluxes (most likely wetland and biomass burning CH_4 emissions) around Behchoko and Inuvik in Northwest Territory, the western Canadian Arctic. The local signals of atmospheric CH_4 also allow inverse models to optimise biomass burning CH_4 flux (emissions due to forest fire), separately from the remaining/natural CH_4 fluxes (including wetland, soil sink and anthropogenic, but mostly due to wetland CH_4 emissions).

The estimated mean total CH_4 annual flux for the Canadian Arctic is 1.8 ± 0.6 $TgCH_4$ yr^{-1} (wetland flux is 1.5 ± 0.5 $TgCH_4$ yr^{-1}, biomass burning flux 0.3 ± 0.1 $TgCH_4$ yr^{-1}). The mean total flux in this study is comparable to another regional flux inversion result of 2.14 $TgCH_4$ yr^{-1} by Thompson et al. (2017), but much higher than the global inversion result of 0.5 $TgCH_4$ yr^{-1} by CarbonTracker-CH_4 (Bruhwiler et al., 2014). The strong regional CH_4 signals at INU and BCK appear to yield flux estimates in this study with narrower high summer emission period and lower wintertime wetland emission compared with the estimates by Thompson et al. (2017).

Clear inter-annual variability is found in all the estimated summertime natural CH_4 fluxes for the Canadian Arctic, mostly due to Northwest Territories. These summertime flux variations are positively correlated with the surface temperature anomaly ($r = 0.55$). This result indicates that the hotter summer weather condition stimulates the wetland CH_4 emission.

With longer data records and more analysis in the Arctic, inversion CH_4 flux estimates could yield more details on CH_4 emission strength and seasonal cycle (onset and termination of wetland emissions), and dependence of wetland fluxes on climate conditions. More knowledge on the flux and climate relationship could help evaluate and improve bottom-up wetland CH_4 flux models.

Next, we will perform a similar study for the CO_2 measurements from these sites to estimate the Canadian Arctic CO_2 fluxes. Estimation of CO_2 and CH_4 fluxes and monitoring how these fluxes change in the future will improve our understanding on the response of the Arctic carbon cycle to climate change, and also yield long-term trends in CO_2 and CH_4 emissions in the Canadian Arctic.

Reply to Comments by Referee #2

We thank the referee for constructive and helpful comments to improve our manuscript with more clarifications. We address the comments (italic and red). In the responses, we also indicate the changes made in the manuscript (in blue font).

General comments

This manuscript presents atmospheric observations of CH4 from 5 new in-situ measurements sites in the Canadian Arctic and uses these (plus one other site) in atmospheric inversions to determine the land-atmosphere flux of CH4. The authors find notable inter-annual variability in the natural (wetland) flux, which may be related to variations in surface temperature. Although the study is interesting and fairly well presented, further explanations and clarifications for some of the methods are needed before being published. In addition, minor technical corrections for English language usage are required.

We report the modifications and additional explanations that we made in the manuscript.

Specific comments

P1, L14: I suggest specifying the number, instead of "multiple". Also how is "inversion modelling system" defined, by the inversion algorithm or transport model used? In this study 2 different transport models were used with 3 different meteorological datasets, so I suggest the authors state this instead.

As suggested, we have changed the sentence more specifically:

From:

Multiple regional Bayesian inversion modelling systems are applied..

To:

Three regional Bayesian inversion modelling systems with two Lagrangian Particle Dispersion Models and three meteorological datasets are applied…

P1, L30: I suggest the authors state what the carbon is vulnerable to, i.e., conversion to CH4 and CO2 which can be emitted to the atmosphere

After "vulnerable", we have added "to conversion to CH_4 and CO_2 which can be emitted to the atmosphere".

P2, L5: Please specify the magnitude of what, presumably CH4 emission but this should be stated

Yes, it is the magnitude of CH_4 emission. We have changed to:

"… show large discrepancies in the spatial distribution of wetland CH_4 source, as well as its magnitude"

P3, L7 (and throughout): It's actually CH4 volume mixing ratio that is reported, and not concentration, so I suggest changing "concentration" to "mixing ratio" throughout.

As the referee noted, gaseous concentration is frequently referred to as 'volume mixing ratio'. We have changed from "concentration" to "mixing ratio", throughout the manuscript.

P5, L31: By "SD of the observed time series to their fitted curves" do the authors mean the SD of the residuals, i.e., after subtracting the fitted curves? This is not clear.

Yes, we mean SD (standard deviation) of the residual of the observations from a fitted curve. That is also referred residual standard deviation. For clarification, we have added "residual" into the sentence:

"monthly Standard Deviation (SD) of the residual of observed time series..."

P5, L34 to P6, L2: This needs some explanation why the difference between SD_PM and SD_24 gives an indication of whether the daily variability is due to local scale changes in emissions or seasonally changing atmospheric transport. I guess the authors mean that SD_24, which includes also night-time data, is more sensitive to local emissions than SD_PM, but an explanation should be provided.

We use the difference between SD_PM and SD_24 as an indication of local emission. SD_24 includes nighttime data which is more sensitive to local emissions than SD_PM. For clarification, we have added the following sentences:

The nighttime planetary boundary layer (PBL) is usually shallow, while the daytime boundary layer is usually deeper and well mixed. If there are local CH_4 sources, the emission is mixed into a shallow PBL at night (yielding higher mixing ratio) and deeper PBL during the day (yielding lower mixing ratio). The resultant diurnal variations in the CH_4 mixing ratios are evident as larger CH_4 SD_24 compared to SD_PM. In the absence of local sources, SD_24 is comparable to SD_PM.

P6, L6: "rectified" is not the right term here (the rectifier effect is a specific term given to the co-variation of flux and planetary boundary layer height, particularly for CO2, which doesn't apply here). Instead use "amplified".

As the referee suggested, "amplified" is more suitable than "rectified". We have revised the text accordingly.

P10, L7: The authors should change this sentence to either "Our Bayesian inversion optimizes…" or "The Bayesian inversion used here optimizes…" to make it clear that the approach used here is not the only approach.

We have changed:

From: "The Bayesian inversion optimises…"

To : "The Bayesian inversion used here optimises…"

*P10, L16: The authors state that the matrix **K** is the product of **M** (the footprints) and **x** (the surface fluxes) and is a Jacobian matrix of flux sensitivities. The elements of **K** must be in mass mixing ratio units (i.e. the same units as **y**), so by definition this is not a Jacobian matrix (but **M** is a Jacobian). Also, the dimensions of **M** and **x** should be given.*

As the referee noted, our usage of 'Jacobian matrix of flux sensitivities' is not correct. To avoid confusion, we have removed the term "Jacobian matrix" from the sentence and revised with the addition of the dimensions of $\boldsymbol{M}$ and $\boldsymbol{x}$. The text has been changed:

From:

$\boldsymbol{K}$ is the matrix of contributions from R sub-regions. $\boldsymbol{K}$ is a Jacobian matrix of flux sensitivity, a product of two matrices, $\boldsymbol{M}$ and $\boldsymbol{x}$. $\boldsymbol{M}$ is the modelled transport (or footprints in this study), and $\boldsymbol{x}$ is the spatial distribution of the surface fluxes.

To :

$\boldsymbol{K}$ (N×R) is the matrix of contributions on the observations (N) from all the fluxes (R) of sub-regions. $\boldsymbol{K}$ is a product of two matrices, $\boldsymbol{M}$(N × LL) and $\boldsymbol{x}$ (LL×R), $\boldsymbol{M}$ is the modelled transport (or footprints in this study), and $\boldsymbol{x}$ is the spatial distribution of the surface fluxes. LL (=LAT×LON) is the dimension of our domain (1°x1° in latitudes (LAT) by longitudes (LON)).

P10, L22: The units of the observation uncertainty should be specified, presumably this is ppb. Also, an explanation should be given of how the value of 0.33 was derived, especially as this seems rather small. Furthermore, an estimate of the appropriateness of the uncertainty estimates should be given, e.g. the value of the reduced-chi-square statistic.

The 33% (0.33) prior model-data mismatch is comparable to other regional inversion studies (e.g. Gerbig et al. (2003), Zhao et al. (2009)). Zhao et al. (2009) included uncertainties from LPDM dispersion, wind field, aggregation and background mixing ratio to estimate prior model-data mismatch uncertainty. However such estimate has many assumptions that are difficult to evaluate. In this study, we tested the sensitivity of the inversion results to this setting by using 33% and 66%, as the model-data mismatch errors. The posterior fluxes changed by less than 5% for all sub-regions (and the different sub-region masks), indicating that the flux estimates were not highly sensitive to the prior error specification.

In response to a similar comment from referee 1, we have added more details (in blue below) to clarify page 10, lines 23-24:

'We examined the inversion's sensitivity to these uncertainties by doubling their values. The posterior fluxes changed by less than 5% for all sub-regions (and the different sub-region masks). The results showed the optimised fluxes are not strongly dependent on these prescribed uncertainties.'

In statistical error analysis, the reduced chi-square test qualitatively measures the goodness of fit of the model to the observations (Hughes and Hase, 2010, Drosg (2009)). In the limit of infinite number of data points and the data are independent and normally distributed, the value of reduced chi-square should be 1. Following Drosg (2009), the reduced chi-square is given by:

$$reduced\ \chi^2 = \frac{1}{N}\sum_k \sum_j {\chi_{jk}}^2$$

Where chi-square is:

$${\chi_{jk}}^2 = \frac{\sum_i \left(model_{ijk} - obs_{ijk}\right)^2}{{\sigma_{jk}}^2}$$

$$obs = observation - model_{background}$$

$$\sigma_{jk} = standard\ deviation\ \ of\ observation\ for\ month\ j\ at\ site\ k$$

$$i = 1, n_{jk}\ (number\ of\ observation\ for\ month\ j\ at\ site\ k)$$

$$The\ estimsted\ degrees\ of freedom\ N\text{:}$$

$$N = \left(\sum_k \sum_j n_{jk}\right) - (fluxes\ per\ region \times number\ of\ region \times number\ of month)$$

The overall reduced chi-squares for our experiments are:

	Mask A	Mask B	Mask C
	YT, NT, NU	YT+NT, NU	YT+NT+NU
FLEXPART_EI	1.244	1.237	1.262
FLEXPART_JRA55	1.236	1.234	1.245
WRF-STILT	1.255	1.249	1.266

Given that the observations are not normally distributed (more frequent high and very high mixing ratio events than low mixing ratio events) and the limited amount of observations, there does not seem to be a strong reason to reject the model results.

We have added a paragraph on the assessment (evaluation) of our model results with reduced chi-square statistics in Section 4.6 [Comparison of modelled and observed mixing ratios (formerly Section 4.5. Comparison of prior and posterior concentrations to observations)]:

Another qualitative measure of the goodness of fit of the model to the observations is the reduced chi-square statistics (Drosg., M., 2009;. Hughes, I. G. and T. Hase, 2010). In the limit of infinite number of data points and the data are independent and normally distributed, the value of reduced chi-square should be 1. The overall reduced chi-squares for all our experiments are in a narrow range of 1.23─1.27. Given that the observations and modelled mixing ratios are not normally distributed (more frequent high and very high mixing ratio events than low mixing ratio events) and the limited amount of observations, there does not seem to be a strong reason to reject the model results

P10, L29-30: This needs a bit more explanation, do the authors mean that they have separate variables for the biomass burning and other emissions, which are optimized simultaneously. In this case, the total number of variables would be R x 2 x number of flux time steps.

Yes, R should be the number of all fluxes to be solved. We solved two fluxes (biomass burning and other missions) per sub-region. We have changed the sentence (note: originally on page 10, lines 14-15):

From : R is the number of sub-regions to be solved.

To : R is the number of fluxes to be solved. R is two fluxes per sub-region × number of sub-regions (i.e., 2 to 6 in this study).

Section 3.3.2: Using only 3 regions for the optimization represents a significant aggregation error, as it is assumed that both the spatial pattern and relative magnitudes of the fluxes within each region are correct. Why was the inversion performed only for these coarse regions? Other than being different territories, are they characterized by having similar ecosystems, climate or other?

We tried to account for the potential errors in the spatial pattern and relative magnitudes of the fluxes by using three different priors to provide a range of spatial and flux magnitude patterns. In our results, the prior flux error is smaller than the model transport error (as estimated by the different transport models used in this study).

The number of sub-regions that could be resolved by the inversion depends mainly on the amount of observations (spatial coverage density and strength of regional signals above the background variations) and magnitudes of the transport errors. In the absence of transport errors, the inversion can resolve a large number of sub-regions (an order of magnitude more in some experiments we tried). But with the present transport model errors, we begin to see unrealistic (negative fluxes) in weak flux region (Yukon) sporadically in our results. Hence, observations and model errors limit the number of sub-regions used in the inversion. The regions were defined based mainly on the geographical characteristics. Yukon has many mountains and little wetlands. Northwest Territories is mainly lowlands

with most of the wetland in the Canadian Arctic. Nunavut is a part of the Canadian Shield or Laurentian Plateau with limited wetlands.

Section 3.3.3: Errors in the modelled background can incur errors in the posterior fluxes. Did the authors check their global modelled CH4 mixing ratios (from NIESTM) with independent observations in the northern high latitudes? Was an estimate of the uncertainty in the background made and included in the overall observation uncertainty?

Yes, we checked the performance of NIES-TM with the independent observations. Here, we showed the comparison of model and observations for the sites, Alert, Barrow and Cold Bay, which were not used for the inversion in this study. Overall, the model captures the observed variations at synoptic scale to seasonal and long-term trend.

Yes, in our inversion, background uncertainty is implicitly included in observation error as we mentioned in the earlier response.

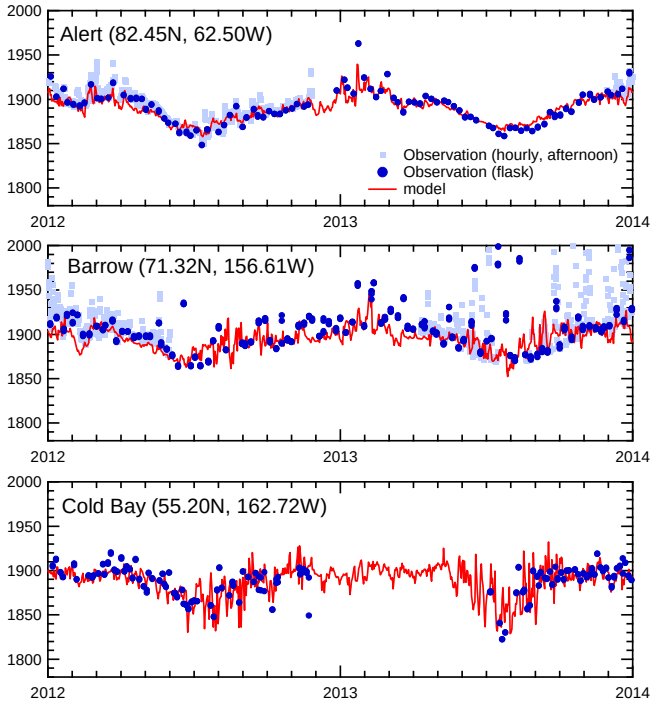

P12, L21: The sub-region masks A to C are not defined in the text

The sub-regions are defined in the earlier section 3.3.2. But the masks A, B and C have not been stated in the text, thought they are illustrated in Fig. S4. The sentence in Section 3.3.2 have been changed:

From:

We set up three sub-region masks for the Canadian Arctic based on three territories 1) Northwest Territories (NT), Yukon (YT), and Nunavut (NU), as shown in Fig. S4

To:

For the Canadian Arctic based on three territories, Northwest Territories (NT), Yukon (YT), and Nunavut (NU), we set up three sub-region masks, Mask A, B and C, as shown in Fig. S4.

P12, L26: I suggest the authors state that the negative biomass burning fluxes are "spurious" since the biomass burning source cannot be negative.

We have modified by adding a sentence as suggested:

As a result, negative mean fluxes, i.e. CH_4 sinks, could appear, especially in YT (Fig. 8a); the negative biomass burning fluxes are "spurious" since the biomass burning CH_4 source cannot be negative. However, a null-flux would be consistent within error bars.

P15, L18-19: Do the authors mean the anomalies of the deseasonalised data? It is important to look at the anomalies in the data after the mean seasonality has been subtracted to avoid correlations with temperature between months, which would override possible correlations with temperature between years.

Yes, the anomalies of fluxes and meteorological parameters we discussed there are the de-seasonalised data by subtracting the 4-year averaged monthly mean values. .

Figure 12: It would be interesting to see the regressions for the prior wetland emissions as well. How strongly are the prior wetland emissions correlated with the meteorological variables and how does this influence the posterior correlations?

In our study, natural CH_4 fluxes (wetland and other fluxes except biomass burning CH_4 flux) in prior emission cases, C1 and C2, are multi-year mean monthly fluxes. Therefore they have no year-to-year anomalies and no correlation with the meteorological anomalies. Only for C3, the prior wetland CH_4 fluxes from WetCHARTs ensemble mean exhibit inter-annual variation, the correlations with temperature and precipitation anomalies are $r = 0.34$ and $r = 0.92$ respectively.

The table below shows the correlation coefficients of the natural (wetland) posterior fluxes and the meteorological variables for individual emission scenarios along with the correlation coefficients of the prior natural fluxes. The posterior natural fluxes in C3 with WetCHARTs prior fluxes show slightly higher correlations than those in the other two cases with cyclo-stationary prior fluxes. But overall there is no significant dependency of posterior correlation on the prior wetland fluxes. This result indicates that the inter-annual variations in the posterior wetland fluxes are mainly determined by the observations, rather than by the prior fluxes. Note that as following Referee 1's suggestion, we have changed C1, C2 and C3 to VIS, GEL, and WetC respectively.

	Natural			
	temperature		precipitation	
	prior	posterior	prior	posterior
C1 (VIS)	0.00	0.55	0.00	0.11
C2 (GEL)	0.00	0.54	0.00	0.07
C3 (WetC)	0.26	0.55	0.90	0.16

In the revision, we have added texts to explain the prior flux influence on the posterior flux-climate correlations in the section of "Relationship of fluxes with climate anomalies (now in Section 4.5).

In prior cases VIS and GEL, natural CH_4 fluxes (wetland and other fluxes except biomass burning CH_4 flux) are multi-year mean monthly fluxes. Therefore these prior fluxes have no year-to-year anomalies and no correlation with the meteorological anomalies. Only in WetC, the prior with wetland CH_4 fluxes from WetCHARTs ensemble mean exhibits inter-annual variations, the correlations with temperature and precipitation anomalies are r = 0.26 and r = 0.90 respectively. The posterior natural fluxes with WetC show slightly higher correlations (r= 0.55 with temperature, r=0.16 with precipitation) than the mean correlation values. But, overall there is no clear dependency of posterior correlations on the inherent climate anomaly correlations in the prior fluxes. This result indicates that the inter-annual variations in posterior wetland fluxes in this study are mainly determined by the observations, rather than by prior fluxes.

Technical comments

P1, L26: "stronger then" should be "stronger than"

Corrected.

P1, L27: add "from" before "about 722 pbb"

Added "from"

Generally: attention should be paid to the use of articles "the" and "a" and when no article should be used at all.

Thank you for your comment, we reviewed the text and tried to correct the usage of articles.

P6, L14: replace "Like" with "Similar to" as "like" in this sense is very colloquial.

Changed from "Like" to "Similar to"

P6, L15: there are words missing in this sentence, it should be "…indicates that there is a weaker local source of CH4…" and "than around the three continental sites".

Corrected, by adding the words as follows:

This indicates that there is a weaker local source of CH_4 around CBY than around the three continental sites.

P6, L19: should be "suggested that there are on-going CH4 emissions from…"

Changed:

From: suggested the CH_4 emissions from

To: suggested that there are on-going CH_4 emissions from

P6, L29: should be "due to the (very) short period of daylight"

Changed:

From: due to limited winter daytime

To: due to the short period of daylight

P8, L27: should be "C3 is the same as used in C2, but…"

Corrected.

P9, L31: should be "…map of climatological termite emissions"

changed

From: a climatological emission map of termite"

To: map of climatological termite emission"

P12, L16: change "done" to "made"

Changed.

P12, L22: should be "are shown" (not "showed")

Corrected.

Fig. 5: should be "same as C2"

Corrected.

P14, L25: Suggest changing the section heading to "Sensitivity tests" since there are more than one

As suggested, we changed the section heading:

From: Sensitivity test

To: Sensitivity tests

P15, L7: should be "in winter compared to…" (not "against") and I think the authors mean "which might contribute to large uncertainties in the flux estimation"

We have changed:

From: in winter against the observed concentrations, which might have large uncertainties in flux estimation.

To: in winter compared to the observed CH_4, which might contribute to large uncertainties in flux estimation.

P15, L9: change "done" to "made"

Changed.

References:

Drosg., M., Dealing with Uncertainties: A Guide to Error Analysis , Second Edition Manfred Drosg Springer, 2009.

Gerbig, C., J. C. Lin, S. C. Wofsy, B. C. Daube, A. E. Andrews, B. B. Stephens, P. S. Bakwin, and C. A. Grainger, Toward constraining regional-scale fluxes of CO_2 with atmospheric observations over a continent: 1. Observed spatial variability from airborne platforms, J. Geophys. Res., 108, 4756, doi:10.1029/2002JD003018, D24, 2003.

Hughes, I. G. and T. Hase, Measurements and their Uncertainties: A Practical Guide to Modern Error Analysis Oxford, 2010.

Zhao, C., A. E. Andrews, L. Bianco, J. Eluszkiewicz, A. Hirsch, C. MacDonald, T. Nehrkorn, and M. L. Fischer (2009), Atmospheric inverse estimates of methane emissions from Central California, J. Geophys. Res., 114, D16302, doi:10.1029/2008JD011671, 2009.

Analysis of atmospheric CH_4 in Canadian Arctic and estimation of the regional CH_4 fluxes

Misa Ishizawa[1], Douglas Chan[1], Doug Worthy[1], Elton Chan[1], Felix Vogel[1] and Shamil Maksyutov[2]

[1]Environment and Climate Change Canada, Toronto, M3H 5T4, Canada
[2]National Institute for Environmental Studies, Tsukuba, 305-8506, Japan

Correspondence to: Misa Ishizawa (misa.ishizawa@canada.ca)

Abstract. The Canadian Arctic (>60˚N, 60˚W–141˚W) has the potential for enhanced atmospheric methane (CH_4) source regions as a response to the ongoing global warming. Current bottom-up and top-down estimates of the regional CH_4 flux range widely. This study analyses the recent observations of atmospheric CH_4 from five arctic monitoring sites and presents estimates of the regional CH_4 fluxes for 2012–2015. The observational data reveal sizeable synoptic summertime enhancements in the atmospheric CH_4 that are clearly distinguishable from background variations, which indicate strong regional fluxes (mainly wetland and biomass burning CH_4 emissions) around Behchoko and Inuvik in the western Canadian Arctic. ~~Multiple~~ Three regional Bayesian inversion modelling systems with two Lagrangian Particle Dispersion Models and three metrological datasets are applied to estimate fluxes for the entire Canadian Arctic and show relatively robust results in amplitude and temporal variations even across different transport models, prior fluxes and sub-region masking. The estimated mean total CH_4 annual flux for the Canadian Arctic is 1.8 ± 0.6 $TgCH_4$ yr^{-1}. The flux estimate in this study is partitioned into biomass burning, 0.3 ± 0.1 $TgCH_4$ yr^{-1}, and the remaining natural (wetland) flux 1.5 ± 0.5 $TgCH_4$ yr^{-1}. The estimated summertime natural CH_4 fluxes show clear inter-annual variability that is positively correlated with surface temperature anomalies. This indicates that the hot summer weather conditions stimulate the wetland CH_4 emissions. More data and analysis are required to statistically characterise the dependence of regional CH_4 fluxes on climate in the Arctic. These Arctic measurement sites should help quantify the inter-annual variations and long-term trends in CH_4 emissions in the Canadian Arctic.

1 Introduction

Atmospheric methane (CH_4) is one of the principal greenhouse gases with a global warming potential (GWP), 34 times stronger ~~then~~ than carbon dioxide (CO_2) over a time period of 100 years, and 96 times over 20 years (Gasser et al., 2017). The atmospheric CH_4 level has increased to twice the level of the pre-industrial era, from about 722 ppb to 1803 ppb in 2011 (Ciais et al., 2013). The Arctic natural/wetland CH_4 emission is an area of interest as it is a potentially growing CH_4 source under climate change (AMAP, 2015). The Arctic is mainly continuous permafrost that contains large quantities of soil carbon, ~1700 PgC, (Tarnocai et al., 2009), which is highly vulnerable to conversion to CH_4 and CO_2 which can be emitted to the atmosphere under the globally warming climate. However, there is only ~~a~~ low confidence in the exact magnitude of CO_2 and CH_4 emissions caused by the carbon lost and whether the thawing carbon will decompose aerobically to release CO_2 or anaerobically to release CH_4 (~~Ciais et al. 2013)~~ e.g.

McGuire et al., 2009; Schuur et al., 2015; Thornton et al., 2016). ~~Overall, the natural CH_4 flux estimates remain largely uncertain in higher northern latitudes (Kirschke et al., 2013;Saunois et al., 2016).~~

~~Bottom-up estimates from wetland methane models in WETCHIMP, some of which are also used for fundamental climate change research within the Coupled Model Intercomparison Phase 6 (CMIP6), show large discrepancies in the spatial distribution of wetlands, as well as the magnitude (Melton et al., 2013). The wetland models define the extent of existing ecosystems and wetland extents from ground based inventory and/or space based information. In the higher latitudes, the limited ground based information has hindered the mapping of wetland. Recently, remote sensing has been providing more information, but the high latitude wetland extent still has large uncertainties (Olefeldt et al., 2016;Thornton et al., 2016).~~

~~In addition to uncertainty in wetland extent, other factors affecting high latitude wetland emissions in different models still remain. A recent inter comparison of CH_4 wetland models (Poulter et al., 2017) in which all models used the same wetland extent, Surface Water Microwave Product Series (SWAMPS) (Schroeder et al, 2015) with Global Lakes and Wetland Database (GLWD) (Lehner and Döll, 2004) and same meteorological data (CRU-NCEP v4.0 reconstructed climate data) to drive their models showed a range in estimated CH_4 emission for North American Boreal/Arctic region which remains larger than that for other regions in the world. This large range of the CH_4 emissions for North American Boreal/Arctic region indicates the uncertainty in our current understanding of physical and biogeochemical processes that contribute to wetland CH_4 emissions.~~

The natural CH_4 flux estimates remain largely uncertain in higher northern latitudes. There have been many studies on CH_4 emission using bottom-up and top-down methods and Saunois et al. (2016) provide a thorough review of the different studies. In general, ~~the~~ bottom-up flux estimates for the northern high latitudes from biogeochemical CH_4 models have large variations, and the mean estimate is much higher than ~~the~~ top-down estimates from the inverse modelling (Saunois et al., 2016). For the Boreal North America region including Alaska and the Hudson Bay Lowlands (HBL, the second largest boreal wetland in the world), the bottom-up mean estimate is ~32 $TgCH_4\ yr^{-1}$, with a wide range from 15 to 60 $TgCH_4\ yr^{-1}$. On the other hand, the top-down estimate is ~12 $TgCH_4\ yr^{-1}$ with a narrower range from ~7 to 21 $TgCH_4\ yr^{-1}$.

Bottom-up estimates from wetland methane models in WETCHIMP show large discrepancies in the spatial distribution of wetlands~~~~ CH_4 source, as well as its magnitude (Melton et al., 2013). In the higher latitudes, the limited ground-based information has hindered the mapping of wetland. Recently, remote sensing has been providing more information, but the high-latitude wetland extent still has large uncertainties (Olefeldt et al., 2016;Thornton et al., 2016). In addition to uncertainty in wetland extent, other factors affecting high-latitude wetland emissions in different models still remain. A recent inter-comparison of CH_4 wetland models (Poulter et al., 2017) in which all models used the same wetland extent, Surface Water Microwave Product Series (SWAMPS) (Schroeder et al., 2015) with Global Lakes and Wetland Database (GLWD) (Lehner and Döll, 2004) and same meteorological data (CRU-NCEP v4.0 reconstructed climate data) to drive their models showed a range in estimated CH_4 emission for North American Boreal/Arctic region which remains larger than that for other regions in the world. This large range of the CH_4 emissions for North American Boreal/Arctic region indicates the uncertainty in our current understanding of physical and biogeochemical processes that contribute to wetland CH_4 emissions.

Top-down atmospheric inverse ~~modelling~~ models have been developed to infer~~s~~ the ~~CH_4~~ fluxes with observed atmospheric CH_4 ~~concentrations~~ mixing ratios as constraint. ~~using different optimizations, including Bayesian, (e.g. Thompson et al., 2017; Lin et al., 2003), 4D variational optimization (4Dvar) (e.g. Bergamaschi et al., 2013; Bousquet et al., 2011), ensemble Kalman filter (EnKF) (e.g., Bruhwiler et al., 2014), Geostatistical (e.g., Michalak et al., 2004;Miller et al., 2014). Inversion models also employ different atmospheric transport models and prior (bottom-up) fluxes as constraints. .~~ Global CH_4 inversion studies estimate global distribution of emissions and sinks from observation sites around the world and/or space (e.g. Bousquet et al., 2011; Bergamschi et al., 2013; Bruhweiler et al, 2014), but with limitted observational infromation in higher northern latitudes. Recently ground-based observation coverage in high northern latitudes has been improving, including towers and aircraft measuerments (e. g., Karion et al. 2016; Sasakawa et al 2010.; Chang et at., 2014). These observations have been used for CH_4 flux estimation in specific regions. For North America, previous atmospehric CH_4 studies were mainly focused on Alaska (e.g., Miller et al., 2016; Hartery et al. 2018). Thompson et al., (2017) conducted CH_4 flux estiamte for entire region north of 50˚N, combining recent high-latitude surface observations. Estimated CH_4 emissions for the Canadian Arcitc show disctipancies among the inverse studies; the mean total CH_4 emission (2006-2010) is ~1.8 $TgCH_4$ by TM5-4DVAR (Bergamschi et al., 2013), 0.5 $TgCH_4$ by CarbonTracker-CH_4 (Bruhweiler et al, 2014), and 2.1 $TgCH_4$ by FLEXINVERT (Thompson et al., 2017). ~~Therefore,~~ Differences ~~in~~ including model ~~optimisation algorithms/approaches~~,transports ~~and~~ prior fluxes and observational datasets ~~errors and their uncertainties can~~ could affect the inversion results. ~~Furthermore, differences in observational platforms network (e.g. surface measurements, aircraft measurements, remote sensing measurements) and the limited observational information also have impacts on the optimisation of the CH_4 fluxes.~~ The previous CH_4 inversion studies used only Alert in the Canadian Arctic, the most northern site in the world. Several new sites in the Canadian Arctic (described in the next paragraph) might be helpful in constraining flux estimation.

Canada has a large Arctic/sub-Arctic region with wetland and permafrost. It is important to study the methane cycle and monitor the impact of climate change in this sensitive region as it impacts atmospheric CH_4 levels at national, continental and hemispheric scale. Environment and Climate Change Canada (ECCC) has recently added five GHG measurement sites in the north to monitor the time evolution of Arctic GHG and to help constrain flux estimates in the region. In October 2010, ECCC started the measurement at Behchoko (BCK, 115.9˚W, 62.8˚N) that is the first ground-based site of continuous measurement in the Canadian Arctic (representing the land region of Canada north of 60˚N), except for Alert (ALT, 82.5˚N, 62.5˚W) which started in ~~1978~~ 1975. Following BCK, more continuous measurement systems have been installed, Churchill (CHL, ~~82.5˚N, 62.5˚W~~ 58.7N, 93.8W) in 2011, Inuvik (INU, 68.3˚N, 133.5˚W) and Cambridge Bay (CBY, 69.1˚N, 105.1˚W) in 2012. The most recent one is at Baker Lake (BLK, 64.3˚N, 96.0˚W) in July 2017.

This is the first study to ~~present and~~ analyse the atmospheric CH_4 ~~concentrations~~ mixing ratio from the above new ECCC observation sites in the Canadian Arctic region. ~~, and to use the observational information in a regional Bayesian inversion framework to infer the Arctic region CH_4 fluxes. Then the possible linkage of CH_4 fluxes with climate/environmental variations is examined.~~ In this study, we address three key questions: (1) what can the new measurements see from local and regional sources? (2) what are the estimated CH_4 fluxes in the Canadian Arctic from

inverse modelling using these new measurements? and (3) are there any relationship for the Canadian Arctic CH_4 fluxes with climate/environmental variations? This paper is structured as follows: In Section 2, the description of the measurement stations as well as the observational data analyses from daily to inter-annual time scales are given ~~in Section 2~~. Section 3 describes the inversion model framework ~~is described in Section 3~~, and Section 4 presents flux estimates and discusses the flux uncertainties and relationship to climate anomalies. ~~are presented and discussed in Section 4~~.

2 Measurements

ECCC has been operating six measurement sites around the Canadian Arctic region to monitor the GHG ~~concentrations~~ mixing ratios. Alert (ALT) is the most northern GHG monitoring site on the globe since ~~the research laboratory was established~~ weekly flask samples for CO_2 measurement began in 1975. Continuous CH_4 measurement at ALT started in 1988. The other five arctic/sub-arctic sites, Behchoko (BCK), Churchill (CHL), Inuvik (INU), Cambridge Bay (CBY), and Baker Lake (BLK), have become operational gradually since 2007. BLK is the newest site in the Canadian Arctic; the flask air sampling measurement program began in 2014, and continuous measurement started in July 2017. At the four other sites, continuous measurement systems were installed during the period of 2010─2012, and these observational data were used for the inversion in this study. The information of the six measurement sites are in Table 1, and their locations are shown in Fig. 1. Currently, all the ECCC continuous measurements are performed using an in-situ cavity ring-down spectrometer (CRDS, Picarro G1301, G2301 or G2401), and discrete flask air sampling measurements are performed using a gas chromatograph equipped with flame ionisation detectors (GC-FID, Agilent 6890). Both measurements are calibrated against the World Meteorological Organization (WMO) X2004 scale (Dlugokencky et al., 2005). In the following sections, we describe the sites briefly and characterise the observed variations of the CH_4 ~~concentrations~~ mixing ratios at the sites.

2.1 Site Descriptions

Alert (ALT, 82.5^{0}N, 62.5^{0}W) has been referred to as an Arctic background site, being located thousands of kilometres from major source regions. The Alert observatory is ~6 km away from the military base camp. The lack of local source surrounding the site results in no significant diurnal variation in observed atmospheric CH_4 ~~concentrations~~ mixing ratios all year around. In ~~the~~ winter, under weak vertical mixing, well-defined synoptic variations are observed due to inter-continental scale transport along with mainly anthropogenic CH_4 originating from the Eurasia continent (Worthy et al., 2009). The measurements at Alert can represent the large-scale background conditions like long-term trend and mean seasonal cycle in the Arctic (Worthy et al., 2009).

Behchoko (BCK, ~~115.9°W,~~ 62.8°N, 115.9°W) is located on the northwest tip of Great Slave Lake. The continuous measurement was started in October 2012. There is no flask sampling at this site. The air sampling intake is at the top of a 60 m communication tower in a local power generation station; 10 km away from the town of Behchoko, a community ~80 km northwest of Yellowknife, the capital of Northwest Territories. Mixed forests, lakes and ponds surround BCK.

Inuvik (INU, ~~133.5°W,~~ 68.3°N, 133.5°W) is ~120 km south of the coast of the Arctic Ocean. The continuous measurement was started in February 2012, followed by flask sampling in May 2012. The measurement system is located in the ECCC upper air weather station building, 5 km southeast of the town of Inuvik. INU is ecologically surrounded by Arctic tundra and geologically located in the east channel of the Mackenzie Delta where a number of water streams and ponds are formed, and vast hydrocarbon deposits are found. Although there are proposed developments of natural gas and pipeline project, they have been on hold.

Cambridge Bay (CBY, ~~105.1°W,~~ 69.1°N, 105.1°W) is on the southeast coast of Victoria Island. CBY is located ~1 km north of the town of Cambridge Bay, the largest port of the Arctic Ocean's Northwest Passage. Both continuous and flask sampling measurements were started in December 2012.

Baker Lake (BKL, ~~96.0°W,~~ 64.3°N, 96.0°W) is on the shore of Baker Lake, ~320 km inland of Hudson Bay. Weekly flask air sampling has been conducted since June 2014, and the continuous measurement was started in July 2017. The air sampling system is located in the ECCC upper air weather station. As same with INU, BCK is in the midst of Arctic tundra and small lakes.

Churchill (CHL, ~~93.8°W,~~ 58.7°N, 93.8°W) is located on the west coast of Hudson Bay. The GHG monitoring program began with flask air sampling in 2007 before the continuous measurement was initiated in October 2011. The sampling equipment is installed in the Churchill Northern Studies Research Facility, ~23 km east of the town of Churchill. CHL is situated with Arctic tundra to the north and in the northern perimeter of Hudson Bay Lowland, the largest boreal wetland in North America.

2.2 Temporal Variations

Figure 2 shows the time-series of CH_4 ~~concentrations~~ mixing ratios; the hourly-means and their afternoon means (between 12:00─16:00 local time) from continuous measurements, and from flask sampling. The fitted curve and long-term trend to the merged time-series of afternoon mean continuous measurements and flask sampling measurements at each site are also plotted. The curve-fitting method applied to all the merged time series has two harmonics of one-year and a half-year cycles and two low and high pass digital filters with cut-off periods of 4 months and 24 months respectively (Nakazawa et al., 1997).

Overall the features of the continuous and flask measurements are similar regarding long-term trend and seasonal cycle. Compared to the weekly flask sampling measurements, continuous measurements reveal short timescale variations. The diurnal and synoptic ~~concentration~~ variations of atmospheric CH_4 are indications of local and regional scale interactions between the atmosphere and the source fluxes (Chan et al., 2004).

All the sites show similar upward trends of atmospheric CH_4. The growth rates at the Canadian Arctic sites are comparable to the global mean growth provided by NOAA based on the global network (Fig. S1). In 2014, the growth rates jumped at all the sites except BCK. In the following year 2015, the growth rates were lowered, but still

higher than the ones prior to 2014. The rapid enhancement in growth rates at the Canadian Arctic sites is consistent with the globally averaged atmospheric CH_4 (www.esrl.noaa.gov/gmd/ccgg/trends_ch4/). The 2014 growth rate at BCK was also enhanced, but the enhancement was not as high as the other Arctic sites. This moderate growth rate for BCK might be an artefact in its long-term component partially due to a data missing period for two months (mid-November, 2014 to mid-January 2015).

2.2.1 Seasonal and inter-annual variations

Since the long-term trends reflect the global-scale source/sink changes, the long-term component at ALT is subtracted from all the sites to focus on the regional scale features in the observed atmospheric CH_4 data (Fig. 3). The mean seasonal cycles are high in winter and low in summer. The summer minimum is mainly due to strong chemical reaction with OH in the warm season. All are relatively in phase in winter with high peaks around January/February, while the site differences are more noticeable in summer. The summer minimum representative of the large-scale Arctic background condition evident at Alert occurs in July to August. The summer minima at the other Arctic sites could vary considerably as they are the superposition of the enhanced CH_4 sink and increased wetland emissions during warmer seasons. Minima are seen in June at BCK, INU and CHL, followed by BKL and CBY with ~1 to 1.5 month lags. In fact, INU, BCK and CHL have a summer secondary maximum feature (a summer bump), indicative of the influence of local/regional wetland and biomass burning emissions. As seen in Figure 3, these summer bumps are not regular in timing and amplitude, but vary year-to-year. The bumps were observed at BCK, INU and CHL in 2012 which were in phase with each other, but not at any site in 2013. In 2014, a larger summer bump was observed at BCK than 2012 (2014 has strong biomass burning contributions) while the summer bump at CHL was similar to the one in 2012. The cause(s) for the "summer bumps" at BCK, CHL and INU might vary year-to-year, such as local/regional (wetland and forest fires) emission change due to climate anomaly. Other possible cause is inter-annually varying atmospheric transport.

2.2.2 Synoptic and diurnal variability

All measurements of atmospheric CH_4 in the Canadian Arctic show synoptic and daily variations with seasonally changing amplitudes. One quantitative measure of synoptic variability in the observed CH_4 ~~concentrations~~ mixing ratios is the monthly Standard Deviation (SD) of the residual of observed time series to their fitted curves. Figure 4 shows the mean seasonality in SD of all 24 hourly data (SD_24) in CH_4 ~~concentrations~~ mixing ratios at each site except BKL, as well as the mean seasonality of the afternoon hourly data (SD_PM). Although SD_24 and SD_PM appear similar (some are almost identical) except during ~~the~~ summer months, the differences between SD_PM and SD_24 give a measure if the daily variability is reflecting a local scale change in emission or rather seasonally changing atmospheric transport processes. The nighttime planetary boundary layer (PBL) is usually shallow, while the daytime boundary layer is usually deeper and well mixed. If there are local CH_4 sources, the emission is mixed into a shallow PBL at night (yielding higher mixing ratio) and deeper PBL during the day (yielding lower mixing ratio). The resultant diurnal variations in the CH_4 mixing ratios are evident as larger CH_4 SD_24 compared to SD_PM. In the absence of local sources, SD_24 is comparable to SD_PM.

The most substantial synoptic variations are observed in summer at all sites except ALT (Fig. 4). This indicates that the major regional CH_4 emissions in the continental Canadian Arctic occur in summer. In winter, the largest synoptic variation is observed at ALT. The synoptic variations are relatively large for the rest of the sites. The wintertime variability might indicate local anthropogenic emission signals ~~rectified~~ amplified under ~~the~~ winter shallow planetary boundary layer (PBL) or strong long-range transport from other regions which has been demonstrated for ALT (Worthy et al., 2009).

The diurnal variability of atmospheric CH_4 is mainly caused by a local CH_4 emission signal modulated by daily PBL development, or a temporal change of the local source. In the summer, the SD_24 values are higher by > 5ppb than the SD_PM except for ALT. The larger SD_24 in the summer supports the existence of local CH_4 sources around the sites, likely wetland CH_4 emissions. In contrast, the fact ALT has identical SD_24 and SD_PM all year round confirms that there is no significant local source at ALT as mentioned earlier

~~Like~~ Similar to the three continental sites (BCK, INU, CHL), CBY also shows the maxima of SD_24 and SD_PM in summer, but they remain lower than BCK, INU and CHL, but higher than ALT. This indicates that there is a weaker local source of CH_4 around CBY than around the three continental sites. In the cold season (September to May), the SD_24 and SD_PM at CBY are almost identical to ALT. It is noticeable that the SD_24 and SD_PM at BCK, INU and CHL are still higher than ALT until December. These higher SD_24 and SD_PM values in the first half of the cold season might indicate the CH_4 emissions from the ground. Zona et al. (2016) suggested ~~the~~ that there are on-going CH_4 emissions from the Alaskan Arctic tundra during the "zero curtain" period when the soil temperature is near zero with average air temperature below 0°C until the surface is completely frozen.

The SD_24 and SD_PM for winter to spring (January to May) at INU remain higher than the other sites. Also, SD_24 at INU becomes higher than SD_PM from April, and remains higher over summer. At the other sites, the difference between SD_24 and SD_PM are seen mainly in summer months (June─August). This higher variability in atmospheric CH_4 at INU in winter and spring, when the surrounding wetland ecosystem is inactive, might indicate a strong local CH_4 source, such as anthropogenic CH_4 emission from natural gas well/refinery facilities. During ~~the~~ winter, such local CH_4 signals are amplified by the seasonally calm condition (the mean seasonal cycles of wind speed are shown in Fig. S2 in the Supplemental Information Section) as well as by less vertical mixing under the shallow PBL due to ~~limited winter daytime~~ the short period of daylight in the polar region. Figure S3 shows the deviations (from the fitted curve) of observed hourly and afternoon mean CH_4 at INU and BCK along with the wind speed. For April and May, the difference of deviations between hourly CH_4 and afternoon mean CH_4 becomes larger again after the relatively quiet period. This could indicate the signals of local (anthropogenic) emission around INU are amplified as the PBL diurnal variation starts developing due to longer daytime. Another possible local source for the large spring SD_24 and SD_PM at INU is natural CH_4 emission from lakes and ponds during the spring thaw (Jammet et al., 2015). In contrast, SD_24 and SD_PM at BCK become less as the wind speed becomes higher, indicating a lack of local CH_4 source around BCK in spring.

Since ALT is representative of the Arctic background state in synoptic variability, the difference of SD_24 or SD_PM between ALT and each of other sites gives a measure of the regional source influence to the site. The large

regional source influence signals in summer shown in Figure 4 should be useful in constraining the regional flux estimation modelling in the next sections.

3 Regional inversion model description

To estimate the regional CH_4 fluxes in the Canadian Arctic, we apply a Bayesian inversion approach, based on the backward simulations by Lagrangian Particle Dispersion Models (LPDM). In this study, three different transport models and three prior CH_4 flux distributions were used to help estimate the model uncertainties. The following sections describe the various components of our regional inverse modelling.

3.1 Transport models and meteorological data

LPDMs simulate an ensemble of air-following particles which are released from the measurement sites. The air particles travel backwards in time for 5 days with the wind field. Previous studies (e.g. Cooper et al., 2010; Gloor et al, 2001; Stohl et al, 2009) have shown 5 days are typically sufficient to capture the surface influence to a measurement site from the surrounding region. The backward trajectory is used to calculate the footprints as the integrated residence times the particles spent inside the PBL at a resolution of 1.0°×1.0. We use three different regional model ~~settings~~ setups combining two different LPDMs: FLEXPART and STILT, and three different meteorological data from the European Centre for Medium-range Weather Forecasts (ECMWF), Japanese Meteorological Agency (JMA), and Weather Research and Forecasting model (WRF).

LPDMs simulate local contributions for 5 days prior to the measurements at sites. The background condition of atmospheric CH_4 ~~concentrations~~ mixing ratios at the endpoints of the particles is provided by a global model, National Institute for Environmental Studies-Transport Model (NIES-TM) with global CH_4 flux fields. Below are the details of model ~~settings~~ setups in this study.

3.1.1 LPDM: FLEXPART_EI

The first model ~~setting~~ setup is FLEXible PARTicle dispersion model (FLEXPART) (Stohl et al., 2005) driven by Reanalysis meteorology from the European Centre for Medium-range Weather Forecasts (ECMWF) ERA-Interim (Dee et al., 2011; Uppala et al., 2005). The input meteorological data are at 3-hourly time step and interpolated to 1.0°×1.0° horizontal resolution with 62 vertical layers.

3.1.2 LPDM: FLEXPART_JRA55

The second model ~~setting~~ setup is also FLEXPART, but driven by the Japanese 55-year Reanalysis (JRA55) from Japanese Meteorological Agency (JMA, Kobayashi et al., 2015; Harada et al., 2016). JRA55 is at 6 hourly time step resolution and on TL319 (~0.5625°, ~55 km) horizontal resolution and, has 60 vertical layers. For this study, we used the JRA55 dataset at half the resolution (~1.25°). This model ~~setting~~ setup was used for a global inverse modelling system by Global Eulerian-Lagrangian Coupled Atmospheric Model (GELCA). GELCA is a coupled atmospheric model of NIES-TM and FLEXPART (Ishizawa et al., 2016). The primary meteorological observational data for

JRA55 have been supplied by ECMWF. In addition to the ECMWF data, the observational data obtained by JMA and other sources are also used.

2.1.3 LPDM:WRF-STILT

The third model ~~setting~~ setup uses Stochastic, Time-Inverted, Lagrangian Transport Model (STILT) (Lin et al., 2003; Lin and Gerbig, 2005). The wind fields to drive STILT are from the Weather Research and Forecasting model (WRF) (Skamarock et al., 2008) on 10 km resolutions. Detailed descriptions are found elsewhere (Hu et al., 2018; Miller et al., 2014; Henderson et al., 2015). The footprints are aggregated to 1.0°×1.0° horizontal resolution, similar to the other models in this study. The STILT footprint data are provided from CarbonTraker Lagrange which is a Lagrangian assimilation framework developed at NOAA Earth System Research Laboratory.

3.1.4 Global background model: NIES-TM

The background or initial condition for the LPDMs is obtained by sampling a global model of CH_4 at the 5-day back endpoint locations of the LPDM particles. The global background ~~concentration~~ field of CH_4 mixing ratio is simulated by NIES-TM version 8.1i (Belikov et al., 2013) with the optimised CH_4 fluxes with GELCA-CH_4 inversion system (Ishizawa et al., 2016; Saunois et al., 2016). The GELCA-CH_4 inverse modelling system optimised the monthly CH_4 fluxes for 2000-2015 to assimilate a global network of surface CH_4 measurements available through GAW World Data Center for Greenhouse Gases (WDCGG, http://ds.data.jma.go.jp/gmd/wdcgg). The prior CH_4 fluxes for the GELCA-CH_4 global inversion are also used for the regional inversion in this study as described in the later section. The NIES-TM has 2.5°×2.5° horizontal resolution and 32 vertical layers, driven by JRA55. For the global simulation, the CH_4 loss in atmosphere is included; the stratospheric CH_4 loss and OH oxidation schemes are adapted from a model inter-comparison project "TransCom-CH_4" (Patra et al., 2011).

3.2 Prior fluxes

Three cases of prior emissions, ~~C1~~ VIS, ~~C2~~ GEL and ~~C3~~ WetC, were used as listed in Table 2. Since the global background atmospheric CH4 field is calculated with GELCA-CH4 inversion posterior fluxes, we chose ~~C1 and C2 are from~~ the prior (VIS) and posterior (GEL) fluxes from ~~for the global inversion by~~ GELCA as two cases of prior fluxes in our regional inversion, respectively. Note that the continuous CH_4 mixing ratio data from the new Canadian Arctic sites were not used in the GELCA-CH_4 inversion. In this study, the mean wetland fluxes for the last 5 years of the GELCA global ~~inversion~~ model were used the prior forest fire CH_4 fluxes are detailed in Section 3.2.2. ~~C3~~ The third prior case (WetC) is the same ~~set with C2~~ as GEL, but with wetland CH_4 fluxes from WetCHARTs (a recent global wetland methane emission model ensemble for use in atmospheric chemical transport models). WetCHARTs provide inter-annually varying monthly wetland CH_4 fluxes for this study period. The details of prior fluxes are described in the following sections.

3.2.1 Wetland CH_4 fluxes

We used the monthly CH_4 wetland fluxes from two different models. The first model is Vegetation Integrative Simulator for Trace gases (VISIT) (Ito and Inatomi, 2012). VISIT is a process-based model, using GLWD as wetland extent. Beside wetland CH_4 flux, VISIT calculates soil CH_4 uptake and CH_4 emission through rice cultivation. The wetland fluxes combined with CH_4 fluxes from rice cultivation were optimised through the GELCA-CH_4 global inversion as a natural CH_4 flux. The second model is WetCHARTs version 1.0 (Bloom et al., 2017a). WetCHARTs derives wetland CH_4 fluxes as a function of a global scaling factor, wetland extent, carbon heterotrophic respiration and temperature dependence (Bloom et al., 2017b). We used the ensemble mean fluxes over 18 model sets which are available for 2001-2015, using 1) three global scaling factors, 2) two wetland extents: GLWD and GLOBCOVER, 3) CARDAMOM (the global CARbon Data MOdel fraMework) as terrestrial carbon analysis, and 4) three temperature dependent CH_4 respiration functions. The WetCHARTs horizontal resolution is 0.5˚×0.5˚. The modelled CH_4 fluxes are aggregated into 1.0˚×1.0˚ for this study. Figure 5 shows the spatial distribution of three wetland CH_4 fluxes for the summer months (July-August). Overall they are similar, while WetCHARTs (~~C3~~WetC) has stronger emissions in Northwest Territories than the two wetland fluxes from ~~VISIT (C1~~ VIS and ~~C2~~ GEL~~)~~.

3.2.2 Forest fire CH_4 fluxes

GFAS (Global Fire Assimilation System) v1.2 (Kaiser et al., 2012) provides biomass burning (BB) emissions by assimilating Fire Radiative Power (FRP) from the Moderate resolution imaging Spectrometer (MODIS). The FRP observations are firstly corrected for data gaps and then linked to dry matter combustion rates with CH_4 emission factors. GFAS has a daily temporal resolution and 0.1˚×0.1˚ horizontal resolution. In this study, the daily fire CH_4 emissions are spatially aggregated into 1.0˚×1.0˚ resolutions for the regional inversion, though monthly fluxes were used for the GELCA global inversion.

3.2.3 Anthropogenic Emission

The anthropogenic CH_4 emissions are provided from EDGAR (Emission Database for Global Atmospheric Research) v4.2FT2010 (http://edgar.jrc.ec.europa.eu), except for rice cultivation. EDGARv4.2FT2010 emission which is originally at 0.1˚×0.1˚ resolution is aggregated into 1.0˚×1.0˚. Since the EDGARv4.2FT2010 data are available until 2010, the same values for 2010 are used for the years beyond 2010. The CH_4 emission from rice cultivation was replaced with the one from VISIT-CH_4 and then treated as a part of natural fluxes because there is no rice field in the Canadian Arctic and also in the rest of North American Arctic/Boreal region, the influence of CH_4 emission from rice cultivation in the region of interest in this study is negligible. The difference of the optimised anthropogenic emissions in the Canadian Arctic from the prior by the global GELCA inversion is almost negligible (from 0.0247 $TgCH_4\ yr^{-1}$ to 0.0250 $TgCH_4\ yr^{-1}$). Compared to the wetland emissions, the emissions are substantially smaller and localised (see Fig. 5).

3.2.4 Other natural CH_4 fluxes

For other natural CH_4 fluxes, we used a map of climatological termite emissions ~~map of termite~~ from Fung et al. (1991) and modelled soil uptake from VISIT-CH_4. Because of no termite CH_4 emissions in the Canadian Arctic, termite CH_4 emission has no direct impact, but it is included in global simulation for the background CH_4 mixing ratio ~~concentration~~. The prior soil CH_4 uptake is provided by VISIT-CH_4 as oxidative consumption by methanotrophic bacteria in unsaturated lands. Soil CH_4 uptake has large uncertainty regionally and also globally. Kirschke et al. (2013) reported that the global soil uptake ranges from 9 to 47 $TgCH_4\ yr^{-1}$. In the Canadian Arctic, the VISIT-modelled soil uptake is weak (0.094 $TgCH_4\ yr^{-1}$) but spread widely (Fig. 5). In some parts of the eastern Canadian Arctic, soil uptakes exceed other CH_4 emissions, resulting in negative fluxes/net sink of atmospheric CH_4.

3.3 Inversion Setup

3.3.1 Regional inversion

In this study, we use the Bayesian Inversion approach (Tarantola, 1987; Rogers 2000; Enting, 2002). The Bayesian inversion used here optimises the scaling factors of posterior fluxes by minimising the mismatch between modelled and observed ~~concentrations~~ mixing ratios with constraints and given uncertainties using the cost function (J) minimisation method ~~(Lin et al., 2004)~~.

$$J(\boldsymbol{\lambda}) = (\boldsymbol{y} - \boldsymbol{K\lambda})^{\boldsymbol{T}} \boldsymbol{D}_{\epsilon}^{-1} (\boldsymbol{y} - \boldsymbol{K\lambda}) + (\boldsymbol{\lambda} - \boldsymbol{\lambda}_{prior})^{\boldsymbol{T}} \boldsymbol{D}_{prior}^{-1} (\boldsymbol{\lambda} - \boldsymbol{\lambda}_{prior}) \quad (1)$$

where $\boldsymbol{y}$ (N×1) is the vector of observations (with the background ~~concentration~~ mixing ratio representing the modelled CH_4 signal from 5 days prior to the observation time subtracted, see Section 3.2.4), N is the number of time points times number of stations (N is reduced if observations are missing). $\boldsymbol{\lambda}$ (R×1) is the vector of the posterior scaling factors to be estimated, R is the number of ~~sub-regions~~ fluxes to be solved. R is two fluxes per sub-regions × number of sub-regions (i.e., 2 to 6 in this study). $\boldsymbol{\lambda}_{prior}$ is the vector of the prior scaling factors which are all initialised to 1 for all sub-regions, and $\boldsymbol{K}$ (N×R) is the matrix of contributions on the observations (N) from all the fluxes (R) of sub-regions. $\boldsymbol{K}$ is ~~a Jacobian matrix of flux sensitivity,~~ a product of two matrices, $\boldsymbol{M}$ (N × LL) and $\boldsymbol{x}$ (LL×R), $\boldsymbol{M}$ is the modelled transport (or footprints in this study), and $\boldsymbol{x}$ is the spatial distribution of the surface fluxes. LL (=LAT×LON) is the dimension of our domain (1°x1° in latitudes (LAT) by longitudes (LON)). A linear regularisation term has been added which is the second term on the right-hand side of the equation. $\boldsymbol{D}_{\epsilon}$ and $\boldsymbol{D}_{prior}$ are the error covariance matrices. $\boldsymbol{D}_{\epsilon}$ is the prior model-observation error/uncertainty matrix (N×N) where the diagonal elements are $(\sigma_e)^2$. $\boldsymbol{D}_{prior}$ is the prior scaling factor uncertainty matrix (R×R) where the diagonal elements are $(\sigma_{prior})^2$. We assume that the model-observation mismatch errors are uncorrelated each other and the contributions from the sub-regions are uncorrelated. All the off-diagonal elements in $\boldsymbol{D}_{\epsilon}$ and $\boldsymbol{D}_{prior}$ are assumed to be zero. We assigned σ_e= 0.33 for the model-observation error (Gerbig et al., 2013; Lin et al., 2004, Zhao et al., 2009), and σ_{prior}= 0.30 for the prior uncertainty (Zhao et al., 2009). We examined the inversion's sensitivity to these uncertainties by doubling their values. The posterior fluxes changed by less than 5% for all sub-regions (and the different sub-region masks). The results showed the optimised fluxes are not strongly dependent on these prescribed uncertainties. The estimate for $\boldsymbol{\lambda}$ is calculated according to the expression below ~~(Lin et al., 2004)~~.

$$\boldsymbol{\lambda} = \left(\boldsymbol{K^T D_\epsilon^{-1} K} + \boldsymbol{D_{prior}^{-1}}\right)^{-1}\left(\boldsymbol{K^T D_\epsilon^{-1} y} + \boldsymbol{D_{prior}^{-1}\lambda_{prior}}\right) \quad (2)$$

The posterior error variance-covariance, $\boldsymbol{\Sigma}_{post}$, for the estimates of $\boldsymbol{\lambda}$ is calculated,

$$\boldsymbol{\Sigma}_{post} = \left(\boldsymbol{K^T D_\epsilon^{-1} K} + \boldsymbol{D_{prior}^{-1}}\right)^{-1}. \quad (3)$$

We optimise the CH_4 fluxes from biomass burning and separately the remaining fluxes (consisting of wetland emission, soil uptake and anthropogenic emission) on a monthly time resolution.

3.3.2 Domain/Sub-regions

~~We set up three sub-region masks~~ For the Canadian Arctic based on three territories, ~~1)~~ Northwest Territories (NT), Yukon (YT), and Nunavut (NU), we set up three sub-region masks, Mask A, B and C, as shown in Fig. S4. Outside of the Canadian Arctic is treated as one outer region. Regarding the subdivision of the Arctic region, we examined the sensitivity of the flux estimation to the number of sub-regions. As a starting point, the three territories are treated separately. Secondly, YT is combined with NT. There is no existing measurement site in Yukon and no significant CH_4 emissions in prior fluxes. The inversion results in the next section will show YT could not be reliably constrained as a separate sub-region (model uncertainties made the estimated fluxes in YT fluctuate from positive to negative). As the third region mask, we solve the fluxes for one region representing the entire Canadian Arctic. Like YT, NU is a weak source region, compared to NT, and weak observational constraint might lead to unrealistic flux estimates. This exercise on the subdivision gives insights on the constraining power of the existing measurements. Table 3 shows all the inversion experiments in this study. We perform totally 27 experiments with 3 prior emission cases, 3 different transport models and 3 different sub-region masks.

3.3.3 Atmospheric Measurements

This regional inversion study used the continuous measurements at BCK, INU, CBY, and CHL for the four years, 2012–2015 (Fig. 2). First~~ly~~ the afternoon mean values are calculated by averaging the hourly data over 4 hours from 12:00 to 16:00 local time so that the observations we use in this study are more regionally representative assuming mid-day is in well-mixed planetary boundary layer.~~, and then~~ Second, the modelled background ~~concentrations~~ mixing ratios, which were described earlier, are subtracted from the afternoon means. The ~~concentration~~ differences of mixing ratio between ~~observed~~ observations and background ~~concentrations~~ were input into the regional inversion system as local contributions. The observational data examined in Section 2 have been already pre-screened for possible contaminations due to mechanical/technical problems during sampling /analysing processes. Except for the pre-screening, we did not apply any additional data screening or filtering.

4 Results and Discussions

4.1 Comparison of footprints

Figure 6 shows the mean footprints (mean emission sensitivities) of all 4 sites by the three different LPDMs. There are common features, but there are also noticeable seasonal differences and differences between the models. The

spatial coverage is similar, but the sensitivity to emissions around sites depends on the models. Among the models, STILT shows the strongest sensitivity near the sites, while FLEXPART_JRA55 has the weakest sensitivity. All the footprints near the sites for ~~the~~ winter season are stronger than ~~the~~ summer season. The footprint differences among the models are also more significant. STILT appears to be more localised to the sites. These differences indicate that choosing multiple implementations for the atmospheric transport will allow us to reflect some of the uncertainties introduced to our inversion estimate by transport models.

4.2 Signals in the observations (relative to background)

The regional inversion depends on how well local signals can be detected in the observations. Therefore, we first look at the detectability of local/regional fluxes in the observed atmospheric CH_4 ~~concentrations~~ mixing ratios. If the amplitude of local signals is comparable to the background contribution, estimated regional fluxes would be more uncertain because local signals would be difficult to distinguish from the background contributions. In Section 2, we examined the synoptic variability in observed CH_4 ~~concentrations~~. Here we apply the same procedures to the modelled background CH_4 ~~concentrations~~ for the sites to see if the local synoptic signal is distinguishable from the background CH_4 ~~concentrations~~. Figure 7 shows the mean monthly SD of modelled background CH_4 ~~concentrations~~ to their fitted curves for the case of FLEXPART_EI (other model ~~settings~~ setups are analogous), along with those of observed CH_4 ~~concentrations~~ (SD_PM in Fig. 4) for the 4 sites to be used as observational constraints (BCK, INU, CBY and CHL). In summer, all the SD_PM values of the observations are much larger (up to three times), than the respective background SDs, indicating strong local influence. While, in winter, both the observation SD_PM and the background SD are comparable. Thus, the observations could provide more constraints on the estimated regional fluxes in summer than in winter.

4.3 Comparison of prior and posterior fluxes with different transport models

The inversion experiments outlined in Table 3 were ~~done~~ made to estimate the CH_4 fluxes in the Canadian Arctic using atmospheric observations from the aforementioned five ECCC stations. We calculated the posterior flux estimates as the mean of the fluxes estimated in the 9 experiments in Table 3 (for each set of sub-region masks). The variations in the flux results (Standard Deviation) are used to represent the flux uncertainty due to transport errors (3 transport models) and prior flux errors (3 prior emission cases). This flux uncertainty is larger than the posterior flux covariance uncertainty estimates, Eq. (3). Figure 8 shows the monthly posterior fluxes with sub-region masks A and B. The monthly posterior fluxes with mask C are ~~showed~~ shown in Fig. S5, along with the aggregated fluxes with masks A and B for the entire Canadian Arctic. As shown in Fig.8a, the fluxes in NT are dominant, and all the posterior fluxes in NT show clear seasonal cycle and inter-annual variations that are reflected in the total fluxes for the entire Canadian Arctic (Fig. S5). In contrast, no clear seasonal pattern is found for NU and YT (Figs. 8a and 8b). The inversion model has difficulty optimising the weak flux regions. As a result, negative mean fluxes, i.e. CH_4 sinks, could appear, especially in YT (Fig. 8a); the negative biomass burning fluxes are "spurious" since the biomass burning CH_4 source cannot be negative. However, a null-flux would be consistent within error bars.

Next, the differences and similarities in the inversion results from the three transport models are summarised. The differences in the flux estimates by the three different transport models can be seen in Fig. 9. Figure 9 displays the example of the experiments with Mask B by the three different transport models for YT+NT. FLEXPART_JRA55 tends to estimate higher total fluxes than the other models, resulting in higher emissions by ~0.6 $TgCH_4\ yr^{-1}$ than the average of ~1.8 $TgCH_4\ yr^{-1}$. WRF-STILT tends to yield the lowest estimate among the three models, lower by ~0.5 $TgCH_4\ yr^{-1}$ than the average. The posterior total fluxes by FLEXPART_EI appear to be moderate. In ~~the~~ winter, the FLEXPART-EI fluxes are close to zero, same with WRF-STILT. These results are consistent with their footprints (mean emission sensitivities) in Fig. 6. Higher footprint sensitivities near the sites tend to yield lower posterior fluxes and vice versa.

The inter-model differences in the posterior forest fire fluxes (Biomass Burning, BB) are quite ~~significant~~ noticeable in 2014 that is the extreme fire year in NT. Due to the sporadic nature of the fire events, the differences in transport (transport errors) are evident in the modelled prior ~~concentrations~~ CH_4 mixing ratios (Fig. S6c) and could lead to substantial differences in the posterior fluxes (Fig. 9). The WRF-STILT estimated BB in 2014 appears to be moderate (0.23 $TgCH_4\ yr^{-1}$), similar to in 2013 (~0.3 $TgCH_4\ yr^{-1}$), while the other two models show the highest BB flux estimates (0.55─0.67 $TgCH_4\ yr^{-1}$) in 2014, comparable to the prior flux, GFAS estimates.

In contrast, the inter-annual variability in total posterior fluxes is very similar among all three transport model results (as shown in Figs. 8 and S5). The inter-annual variability in the transport models (an intra-model result) appears to be consistent, yielding similar posterior flux inter-annual variability. Since all three different transport models capture this inter-annual variability, it appears to be a robust feature of the CH_4 source/sink in the Canadian Arctic.

Another robust feature appears to be the similarity in the results for the total Arctic emission with different numbers of sub-regions used in the inversion. The sub-region with strong signals in the prior fluxes (NT) and strong observational constraints (BCK and INU within NT) yielded posterior flux results with small uncertainties, while sub-region with weak signals in the prior fluxes (YT) and weak observational constraint (no observations in YT) yielded large uncertainties in the posterior flux estimates. Weak sub-region like YT could be combined with other sub-region (NT) without strong impact on the inversion results. The temporal variations in the inversion results with different numbers of sub-regions (an intra-model result) seem to be a robust feature also. Given that the strong observational constraints and the strong wetland emissions are both located in the central part of the Canadian Arctic, representing the Canadian Arctic as a single region was able to yield reasonable inversion results.

4.4 Comparison with previous estimates

The estimated fluxes for the entire Canadian Arctic in this study are relatively robust in amplitude and temporal variations even with the different prior fluxes and sub-region masking. The mean estimated total CH_4 annual flux for the Canadian Arctic is $1.8 \pm 0.6\ TgCH_4\ yr^{-1}$. Compared with two previous inversion estimates, our estimate is slightly lower than the mean total flux of 2.14 $TgCH_4\ yr^{-1}$ (average from 2009─2013) inferred by FLEXINVERT regional inversion (Thompson et al. 2017), but much higher than the estimate of 0.5 $TgCH_4\ yr^{-1}$ (average from 2006─2010) from the CarbonTracker-CH_4 global inversion (Bruhwiler et al., 2014) (Fig. 10 a).

All the estimated fluxes are seasonally high around July and August (Fig. 10b). The mean summertime maximum of our estimates is quite consistent with the one by Thompson et al. (2017), but our estimated fluxes have narrow high summer emission period and low wintertime emission compared with the estimates by Thompson et al. (2017). These temporal differences in estimated fluxes might reflect the observational constraints used in the respective inversions. Thompson et al. (2017) employed a similar type of regional inversion but for the entire northern high latitudes (north of 50˚N). Except for the flask measurement data at CHL, none of the Canadian Arctic sites used in this study was included in Thompson et al. (2017). The strong regional CH_4 signals at INU and BCK in this study appear to yield flux estimates with narrower high summer emission period and lower wintertime wetland emission compared with the estimates by Thompson et al. (2017).

The flux estimate in this study is partitioned into biomass burning (BB), 0.3 ± 0.1 $TgCH_4\ yr^{-1}$, and the remaining flux 1.5 ± 0.5 $TgCH_4\ yr^{-1}$. The remaining flux is mainly natural/wetland CH_4 emissions, given that anthropogenic contribution to the total prior fluxes without BB is ~2 % according to the EDGAR prior fluxes. The estimated wetland flux is comparable to the WetCHARTs (wetland) ensemble mean of 1.35 $TgCH_4\ yr^{-1}$ (Bloom et al. 2017a; 2017b).

The estimated summertime natural CH_4 fluxes show clear inter-annual variability. The higher emissions are estimated in 2012 and 2014 in this study, which is similar to the results from Arctic Reservoirs Vulnerability Experiment (CARVE) aircraft measurements over Alaska for 2012 to 2014 (Hartery at al., 2018).

4.5 Relationship of fluxes with climate anomalies

Inter-annual variations of estimated CH_4 fluxes are examined in ~~the relationships of the posterior fluxes with~~ relation to climate parameters ~~are examined~~ here, specifically with surface air temperature and precipitation from NCEP reanalysis (Kalnay et al., 1996). First, monthly mean values at the sub-regions as well as the 4-year mean (2012-2015) for each month are calculated, then ~~to obtain~~ the monthly anomalies are computed from the monthly mean values and ~~from~~ the 4-year mean of the corresponding month ~~s (2012–2015)~~. The temperature and precipitation anomalies are aggregated to the respective regions, NT, YT and NU. On the regional level, climate anomalies in NT and NU are quite similar, though YT is less similar to NT and NU. YT is mainly covered by mountains with little wetland. Furthermore, NT has the largest wetland extent and most of the forest fire emissions in 2012-2015. Thus, we look into the correlation in monthly anomalies of CH_4 fluxes with ~~the~~ summer climate anomalies in NT.

In Fig. ~~12~~11, the inter-annual variability of wetland CH_4 fluxes exhibits a moderate positive correlation with the surface temperature anomaly (r = ~~0.57~~ 0.55) and only weakly correlated with precipitation anomalies (r = ~~0.13~~ 0.11). This indicates that the hotter summer weather condition stimulates the wetland CH_4 emission, and precipitation appears to have a less immediate or no direct impact on wetland conditions. In prior cases VIS and GEL, natural CH_4 fluxes (wetland and other fluxes except biomass burning CH_4 flux) are multi-year mean monthly fluxes. Therefore these prior fluxes have no year-to-year anomalies and no correlation with the meteorological anomalies. Only in WetC, the prior with wetland CH_4 fluxes from WetCHARTs ensemble mean exhibits inter-annual variations, the correlations with temperature and precipitation anomalies are r = 0.26 and r = 0.90 respectively. The posterior natural fluxes with WetC show slightly higher correlations (r=0.55 with temperature, r=0.16 with precipitation) than the mean

correlation values. But overall there is no clear dependency of posterior correlations on the inherent climate anomaly correlations in the prior fluxes. This result indicates that the inter-annual variations in posterior wetland fluxes in this study are mainly determined by the observations, rather than by prior fluxes.

Inter-annual variations of estimated BB CH_4 fluxes show a negative correlation with precipitation (r = ~~-0.47~~ -0.41). Also throughout the fire season (June-September), all estimated BB fluxes negatively correlate with precipitation while the prior BB fluxes appear to have no consistent correlations. The inversion results support that dry condition would enhance the forest fire. The estimated BB fluxes show weakly negative correlation with surface temperature (r = ~~-0.38~~ -0.23) on mid-summer average, but the monthly correlations are fluctuating from r = ~~-0.47~~ -0.40 to r = ~~0.69~~ 0.47 over the fire season. Since the period is limited in this study (2012─2015), these statistical relationships are still not clear. Also, the relationship of CH_4 emissions with climate conditions could be complex and non-linear (with extreme fires events in some years). More data and analysis are required to characterise the dependence of CH_4 fluxes on climate in the Arctic.

~~4.5~~ 4.6 Comparison of ~~prior and posterior concentrations to~~ modelled and ~~observations~~ observed mixing ratios

The model-observation statistical comparison is shown with the Taylor diagrams of correlation coefficients and normalised standard deviation (NSD) by three different transport models for the four Arctic sites (Fig. ~~11~~12) using the inversion results with Mask B and prior flux case ~~C3~~ WetC. At BCK and INU, the correlation coefficients and NSD for each model are improved by the inversion. At these two sites, the observations contain large synoptic signals from the Canadian Arctic wetland and provide strong constraints to the inversions. At INU, the improvement for STILT is noticeable, especially with NSD. This is explained further below. At CBY and CHL, no significant changes between the prior and posterior results are seen. This indicates that the regional flux in the Canadian Arctic only weakly influences CBY and CHL.

Further investigation has been done for INU. Figure S7a shows the time-series of modelled ~~concentrations~~ mixing ratios by the three transport models and the observed ~~concentrations~~ mixing ratio. The Taylor diagrams in Fig. S7b show the results annually and by seasons, summer months (June─September) and winter months (October─May) separately as well as for the entire period together. The modelled ~~concentrations~~ mixing ratios by STILT with the prior fluxes could be much higher than the ~~concentrations~~ mixing ratios by the other two models. That results in the higher prior NSD values, especially in winter season. The inversion was able to improve the results by reducing the fluxes and consequently the posterior NSD.

Another qualitative measure of the goodness of fit of the model to the observations is the reduced chi-square statistics (Drosg., M., 2009;. Hughes, I. G. and T. Hase, 2010). In the limit of infinite number of data points and the data are independent and normally distributed, the value of reduced chi-square should be 1. The overall reduced chi-squares for all our experiments are in a narrow range of 1.23─1.27. Given that the observations and modelled mixing ratios are not normally distributed (more frequent high and very high mixing ratio events than low mixing ratio events) and the limited amount of observations, there does not seem to be a strong reason to reject the model results

~~4.6~~ 4.7 Sensitivity tests

~~4.6.1~~ 4.7.1 Prior fluxes: wetland CH_4 fluxes

Wetland CH_4 emissions are the dominant flux in the Canadian Arctic. To examine how the prior fluxes impact on the posterior fluxes, two inversion experiments were conducted with modified WetCHARTs fluxes. One is 50 % reduced emissions in the Canadian Arctic, and another is 50 % increased emissions in the Canadian Arctic. The results are shown as mean posterior natural fluxes in Fig. S8. Despite the change in wetland prior emissions, all the posterior fluxes are similar to the ones in the control case; the changes in the posterior fluxes are less than 5% annually. This indicates that the posterior fluxes are not very sensitive to the amplitude/strength of prior fluxes.

~~4.6.2~~ 4.7.2 Contributions of background ~~concentrations~~ CH_4 mixing ratios on the posterior fluxes

We used the same background ~~contributions~~ CH_4 mixing ratios for the different transport models, which are calculated using the particle endpoints from FLEXPART_JRA55. The idea of using the same background ~~concentration~~ CH_4 fields is to focus on the impact of local/regional transport contribution on regional inversion, separating from the background contribution.

One notable feature in the background ~~concentrations~~ CH_4 mixing ratios is the relatively large synoptic variability, especially in winter ~~against~~ compared to the observed CH_4 ~~concentrations~~, which might ~~have~~ contribute to large uncertainties in flux estimation. To examine how sensitive the inversion results are to these temporal variations in the background ~~concentrations~~ CH_4 mixing ratios, additional experiments with background CH_4 ~~concentrations~~ with smoothing windows of 5 days, 10 days and 30 days were ~~done~~ made (see Fig. S9a).

The examples of the results are shown in Figs. S9b and S9c. The posterior fluxes are not strongly dependent on the different background ~~concentrations~~ CH_4 mixing ratio. Compared with unsmoothed background case, slightly small values of NSD are found in the model-observation statistical comparison for summer with 30-day smoothing. It seems there are sufficient observations (signal level) above the background ~~concentrations~~ CH_4 mixing ratios (noise level) to constrain the inversion results (Fig. 7).

~~4.6.3 Relationship of fluxes with climate anomalies~~

~~The relationships of the posterior fluxes with climate parameters are examined here, specifically with surface air temperature and precipitation from NCEP reanalysis (Kalnay et al., 1996). First, monthly mean values at the sub-regions are calculated to obtain the monthly anomalies from the 4-year means (2012–2015). The temperature and precipitation anomalies are aggregated to the respective regions, NT, YT and NU. On the regional level, climate anomalies in NT and NU are quite similar, though YT is less similar to NT and NU. YT is mainly covered by mountains with little wetland. Furthermore, NT has the largest wetland extent and most of the forest fire emissions in 2012–2015. Thus, we look into the correlation in monthly anomalies of CH_4 fluxes with the summer climate anomalies in NT.~~

~~In Fig. 12, the inter-annual variability of wetland CH_4 fluxes exhibits a moderate positive correlation with the surface temperature anomaly ($r = 0.57$) and only weakly correlated with precipitation anomalies ($r = 0.13$). This~~

~~indicates that the hotter summer weather condition stimulates the wetland CH_4 emission, and precipitation appears to have a less immediate or no direct impact on wetland conditions.~~

~~Inter-annual variations of estimated BB CH_4 fluxes show a negative correlation with precipitation ($r = -0.47$). Also throughout the fire season (June-September), all estimated BB fluxes negatively correlate with precipitation while the prior BB fluxes appear to have no consistent correlations. The inversion results support that dry condition would enhance the forest fire. The estimated BB fluxes show weakly negative correlation with surface temperature ($r = -0.38$) on mid-summer average, but the monthly correlations are fluctuating from $r = -0.47$ to $r = 0.69$ over the fire season. Since the period is limited in this study (2012–2015), these statistical relationships are still not clear. Also, the relationship of CH_4 emissions with climate conditions could be complex and non-linear (with extreme fires events in some years). More data and analysis are required to characterise the dependence of CH_4 fluxes on climate in the Arctic.~~

5 ~~Summary~~ Conclusions

The Canadian Arctic region is one of the potential enhanced CH_4 source regions related to the ongoing global warming (AMAP, 2015), and earth system models differ in their prediction how the carbon loss there will be split up between CO_2 and CH_4 emissions. Even current bottom-up and top-down estimates of ~~the~~ CH_4 flux in the region vary widely. This study:

1) analysed the measurements of atmospheric CH_4 ~~concentrations~~ mixing ratios that include 5 sites established in the Canadian Arctic by ECCC, to characterise the observed variations and examine the detectability of regional fluxes. And,

2) estimated the regional fluxes for 4 years (2012–2015) with the continuous observational data of atmospheric CH_4, ~~employing a Bayesian atmospheric inversion method with three different sets of Lagrangian particle dispersion model and meteorological data (FLEXPART_EI, FLEXPART_JRA55 and WRF-STILT). In addition to the model variations, inversion experiments included different sub-region masks and prior emissions to investigate their impact on the estimated fluxes and their uncertainties. We~~ and also ~~examined~~ the relationship of the estimated fluxes with the climate anomalies.

The observational data analysis reveals large synoptic summertime signals in the atmospheric CH_4, indicating strong regional fluxes (most likely wetland and biomass burning CH_4 emissions) around Behchoko and Inuvik in Northwest Territory, the western Canadian Arctic. ~~These observational signals are quite distinct from the background signals and could be used for inverse flux estimations.~~ The local signals of atmospheric CH_4 ~~concentration signals~~ also allow inverse models to optimise biomass burning CH_4 flux (emissions due to forest fire), separately from the remaining/natural CH_4 fluxes (including wetland, soil sink and anthropogenic, but mostly due to wetland CH_4 emissions).

~~The inverse flux estimates included three different transport models, three different prior wetland emission datasets and three sub-region definitions to help quantify the uncertainties in the results. For wetland, a spatially distributed and slowly varying CH_4 source, the transport models could repeatedly sample the sources around each site and providing sufficient signals for the inversion model to optimise the fluxes. The estimated wetland flux 1.5 ± 0.5~~

~~$TgCH_4\ yr^{-1}$ for the entire Canadian Arctic is relatively robust in amplitude and temporal variation. The estimated biomass (BB) burning flux is 0.3 ± 0.1 $TgCH_4\ yr^{-1}$ on average, but strongly dependent on the transport models. The large point-like BB emissions with strong temporal (daily) variations near Behchoko coupled with the strong transport model differences near the site yielded very different modelled prior concentrations at the site. Consequently inferred BB flux estimates have large uncertainty (particularly for 2014).~~

The estimated mean total CH_4 annual flux for the Canadian Arctic is 1.8 ± 0.6 $TgCH_4\ yr^{-1}$ (wetland flux is 1.5 ± 0.5 $TgCH_4\ yr^{-1}$, biomass burning flux 0.3 ± 0.1 $TgCH_4\ yr^{-1}$). The mean total flux in this study is comparable to another regional flux inversion result of 2.14 $TgCH_4\ yr^{-1}$ by Thompson et al. (2017), but much higher than the global inversion result of 0.5 $TgCH_4\ yr^{-1}$ by CarbonTracker-CH_4 (Bruhwiler et al., 2014). The strong regional CH_4 signals at INU and BCK appear to yield flux estimates in this study with narrower high summer emission period and lower wintertime wetland emission compared with the estimates by Thompson et al. (2017).

Clear inter-annual variability is found in all the estimated summertime natural CH_4 fluxes for the Canadian Arctic, mostly due to Northwest Territories. These summertime flux variations are positively correlated with the surface temperature anomaly (r = ~~0.57~~ 0.55). This result indicates that the hotter summer weather condition stimulates the wetland CH_4 emission. ~~More data and analysis are required to characterise the dependence of CH_4 fluxes on climate in the Arctic. In the future, these Arctic measurement sites should help quantify the inter-annual variations and~~

With longer data records and more analysis in the Arctic, inversion CH_4 flux estimates could yield more details on CH_4 emission strength and seasonal cycle (onset and termination of wetland emissions), and dependence of wetland fluxes on climate conditions. More knowledge on the flux and climate relationship could help evaluate and improve bottom-up wetland CH_4 flux models.

Next, we will perform a similar study for the CO_2 measurements from these sites to estimate the Canadian Arctic CO_2 fluxes. Estimation of CO_2 and CH_4 fluxes and monitoring how these fluxes change in the future will improve our understanding on the response of the Arctic carbon cycle to climate change, and also yield long-term trends in CO_2 and CH_4 emissions in the Canadian Arctic.

Data availability

The data measured at ECCC sites used in this study are available upon request to Doug Worthy (doug.worthy@canada.ca). The Alert data are also periodically updated to WDCGG, http://ds.data.jma.go.jp/gmd/wdcgg. The model-related data are available upon request to corresponding author.

Author Contributions

MI and DC designed the research and prepared the manuscript. MI performed data analysis and inversion experiments. DW led the measurement programs and collected the observational data. MI, DC and EC provided footprints (potential emission sensitivities) information for inversions. All authors contributed to the discussion and interpretation of the results.

Competing Interest

Authors declare that they have no conflict of interest.

Acknowledgments

We acknowledges CarbonTraker (CT) Lagrange program for providing the WRF-STILT footprint data for our inversion study. CT_Lagrange has been supported by NOAA Climate Program Office's Atmospheric Chemistry, Carbon Cycle, & Climate (AC4) Program and the NASA Carbon Monitoring System. We would like to extend our gratitude to the conscientious care taken by the program technicians, Robert Kessler and Larry Giroux, and IT support provided by Senen Racki. Appreciation is also forwarded to the Northwest Territories Power Corporation (NTPC) for making available their building facility to house our equipment and tower to string our sampling lines. NTPC also provided IT communication to permit access to our equipment and transmission of data.

References

AMAP: Assesment 2015: Methane as an Arctic clilmate forcer, Arctic Monitoring ans Assessment Programme (AMAP), Oslo, Norway, 2015.

Belikov, D. A., Maksyutov, S., Sherlock, V., Aoki, S., Deutscher, N. M., Dohe, S., Griffith, D., Kyro, E., Morino, I., Nakazawa, T., Notholt, J., Rettinger, M., Schneider, M., Sussmann, R., Toon, G. C., Wennberg, P. O., and Wunch, D.: Simulations of column-averaged CO_2 and CH_4 using the NIES TM with a hybrid sigma-isentropic (σ-θ) vertical coordinate, Atmos. Chem. Phys., 13, 1713-1732, 10.5194/acp-13-1713-2013, 2013.

Bergamaschi, P., Houweling, S., Segers, A., Krol, M., Frankenberg, C., Scheepmaker, R. A., Dlugokencky, E., Wofsy, S. C., Kort, E. A., Sweeney, C., Schuck, T., Brenninkmeijer, C., Chen, H., Beck, V., and Gerbig, C.: Atmospheric CH_4 in the first decade of the 21st century: Inverse modeling analysis using SCIAMACHY satellite retrievals and NOAA surface measurements, J. Geophys. Res., 118, 7350-7369, 10.1002/jgrd.50480, 2013.

Bloom, A. A., Bowman, K. W., Lee, M., Turner, A. J., Schreder, R., Worden, J. R., Wedner, R. J., Mcdonald, K. C., and Jacob, D. J.: CMS: Global 0.5-deg Wetland Methane Emissions and Uncertainty (WetCHARTs v1.0), ORNL Distributed Active Archive Center, 2017a.

Bloom, A. A., Bowman, K. W., Lee, M., Turner, A. J., Schroeder, R., Worden, J. R., Weidner, R., McDonald, K. C., and Jacob, D. J.: A global wetland methane emissions and uncertainty dataset for atmospheric chemical transport models (WetCHARTs version 1.0), Geosci. Model Dev., 10, 2141-2156, 10.5194/gmd-10-2141-2017, 2017b.

Bousquet, P., Ringeval, B., Pison, I., Dlugokencky, E. J., Brunke, E. G., Carouge, C., Chevallier, F., Fortems-Cheiney, A., Frankenberg, C., Hauglustaine, D. A., Krummel, P. B., Langenfelds, R. L., Ramonet, M., Schmidt, M., Steele, L. P., Szopa, S., Yver, C., Viovy, N., and Ciais, P.: Source attribution of the changes in atmospheric methane for 2006–2008, Atmos. Chem. Phys., 11, 3689-3700, 10.5194/acp-11-3689-2011, 2011.

Bruhwiler, L., Dlugokencky, E., Masarie, K., Ishizawa, M., Andrews, A., Miller, J., Sweeney, C., Tans, P., and Worthy, D.: CarbonTracker-CH_4: an assimilation system for estimating emissions of atmospheric methane, Atmos. Chem. Phys., 14, 8269-8293, 10.5194/acp-14-8269-2014, 2014.

Chan, D., Yuen C. W., Higuchi, K., Shashkov, A., Liu, J., Chen, J., Worthy, D.: On the CO_2 exchange between the atmosphere and the biosphere: the role of synoptic and mesoscale processes, Tellus, 56B, 194-212, 2004.

Ciais, P., Sabine, C., Bala, G., Bopp, L., Brovkin, V., Canadell, J., Chhabra, A., DeFries, R., Galloway, J., Heimann, M., Jones, C., Le Quéré, C., Myneni, R. B., Piao, S., and Thornton, P.: Carbon and Other Biogeochemical Cycles, in: Climate Change 2013: The Physical Science Basis. Contribution of Working Group I to the Fifth Assessment Report of the Intergovernmental Panel on Climate Change, edited by: Stocker, T. F., Qin, D., Plattner, G.-K., Tignor, M., Allen, S. K., Boschung, J., Nauels, A., Xia, Y., Bex, V., and Midgley, P. M., Cambridge University Press, Cambridge, United Kingdom and New York, NY, USA, 465–570, 2013.

Cooper, O. R., Parrish, D. D., Stohl, A., Trainer, M., Nédélec, P., Thouret, V., Cammas, J. P., Oltmans, S. J., Johnson, B. J., Tarasick, D., Leblanc, T., McDermid, I. S., Jaffe, D., Gao, R., Stith, J., Ryerson, T., Aikin, K., Campos, T., Weinheimer, A., and Avery, M. A.: Increasing springtime ozone mixing ratios in the free troposphere over western North America, Nature, 463, 344, 10.1038/nature08708

Dee, D. P., Uppala, S. M., Simmons, A. J., Berrisford, P., Poli, P., Kobayashi, S., Andrae, U., Balmaseda, M. A., Balsamo, G., Bauer, P., Bechtold, P., Beljaars, A. C. M., van de Berg, L., Bidlot, J., Bormann, N., Delsol, C., Dragani, R., Fuentes, M., Geer, A. J., Haimberger, L., Healy, S. B., Hersbach, H., Hólm, E. V., Isaksen, L., Kållberg, P., Köhler, M., Matricardi, M., McNally, A. P., Monge-Sanz, B. M., Morcrette, J. J., Park, B. K., Peubey, C., de Rosnay, P., Tavolato, C., Thépaut, J. N., and Vitart, F.: The ERA-Interim reanalysis: configuration and performance of the data assimilation system, Q. J. R. Meteorolog. Soc., 137, 553-597, 10.1002/qj.828, 2011.

Dlugokencky, E. J., Myers, R. C., Lang, P. M., Masarie, K. A., Crotwell, A. M., Thoning, K. W., Hall, B. D., Elkins, J. W. and L. P. Steele, L. P.: Conversion of NOAA atmospheric dry air CH_4 mole fractions to a gravimetrically prepared standard scale, J. Geophys. Res., 110, D18306, doi:10.1029/2005JD006035, 2005.

Drosg., M.: Dealing with Uncertainties: A Guide to Error Analysis Springer-Verlag Berlin Heidelberg, 2009.

Enting, I. G.: Inverse Problems in Atmospheric Constituent Transport, Cambridge University Press, Cambridge, UK, 392 pp., 2002.

Fung, I., John, J., Lerner, J., Matthews, E., Prather, M., Steele, L. P., and Fraser, P. J.: Three-dimensional model synthesis of the global methane cycle, J. Geophys. Res., 96, 13033-13065, 10.1029/91JD01247, 1991.

Gasser, T., Peters, G. P., Fuglestvedt, J. S., Collins, W. J., Shindell, D. T., and Ciais, P.: Accounting for the climate–carbon feedback in emission metrics, Earth Syst. Dynam., 8, 235-253, 10.5194/esd-8-235-2017, 2017.

Gerbig, C., Lin, J. C., Wofsy, S. C., Daube, B. C., Andrews, A. E., Stephens, B. B., Bakwin, P. S., and Grainger, C. A.: Toward constraining regional-scale fluxes of CO2 with atmospheric observations over a continent: 2. Analysis of COBRA data using a receptor-oriented framework, J. Geophys. Res., 108, doi:10.1029/2003JD003770, 2003.

Gloor, M., Bakwin, P., Hurst, D., Lock, L., Draxler, R., and Tans, P.: What is the concentration footprint of a tall tower?, J. Geophys. Res., 106, 17831-17840, 10.1029/2001JD900021, 2001

Harada, Y., Kamahori, H., Kobayashi, C., Endo, H., Kobayashi, S., Ota, Y., Onoda, H., Onogi, K., Miyaoka, K., and Takahashi, K.: The JRA-55 Reanalysis: Representation of Atmospheric Circulation and Climate Variability, J. Meteor. Soc. Japan, 94, 269-302, 10.2151/jmsj.2016-015, 2016.

Henderson, J. M., Eluszkiewicz, J., Mountain, M. E., Nehrkorn, T., Chang, R. Y. W., Karion, A., Miller, J. B., Sweeney, C., Steiner, N., Wofsy, S. C., and Miller, C. E.: Atmospheric transport simulations in support of the Carbon in Arctic Reservoirs Vulnerability Experiment (CARVE), Atmos. Chem. Phys., 15, 4093-4116, 10.5194/acp-15-4093-2015, 2015.

He, W., van der Velde, I. R., Andrews, A. E., Sweeney, C., Miller, J., Tans, P., van der Laan-Luijkx, I. T., Nehrkorn, T., Mountain, M., Ju, W., Peters, W., and Chen, H.: CTDAS-Lagrange v1.0: a high-resolution data assimilation system for regional carbon dioxide observations, Geosci. Model Dev., 11, 3515-3536, https://doi.org/10.5194/gmd-11-3515-2018, 2018.

Hughes, I. G., and Hase, T.: Measurements and their Uncertainties: A Practical Guide to Modern Error Analysis, Oxford University Press, New York, 2010.

Ishizawa, M., Mabuchi, K., Shirai, T., Inoue, M., Morino, I., Uchino, O., Yoshida, Y., Belikov, D., and Maksyutov, S.: Inter-annual variability of summertime CO_2 exchange in Northern Eurasia inferred from GOSAT XCO_2, Environ. Res. Lett., 11, 105001, doi:10.1088/1748-9326/11/10/105001, 2016.

Ito, A., and Inatomi, M.: Use of a process-based model for assessing the methane budgets of global terrestrial ecosystems and evaluation of uncertainty, Biogeosciences, 9, 759-773, 10.5194/bg-9-759-2012, 2012.

Jammet, M., Crill, P., Dengel, S., and Friborg, T.: Large methane emissions from a subarctic lake during spring thaw: Mechanisms and landscape significance, J. Geophys. Res., 120, 2289-2305, doi:10.1002/2015JG003137, 2015.

Kaiser, J. W., Heil, A., Andreae, M. O., Benedetti, A., Chubarova, N., Jones, L., Morcrette, J. J., Razinger, M., Schultz, M. G., Suttie, M., and van der Werf, G. R.: Biomass burning emissions estimated with a global fire assimilation system based on observed fire radiative power, Biogeosciences, 9, 527-554, 10.5194/bg-9-527-2012, 2012.

Kalnay, E., Kanamitsu, M., Kistler, R., Collins, W., Deaven, D., Gandin, L., Iredell, M., Saha, S., White, G., Woollen, J., Zhu, Y., Leetmaa, A., Reynolds, R., Chelliah, M., Ebisuzaki, W., Higgins, W., Janowiak, J., Mo, K. C., Ropelewski, C., Wang, J., Roy, J., and Dennis, J.: The NCEP/NCAR 40-Year Reanalysis Project, Bull. Am. Meteorol. Soc., 77, 437-471, 1996.

Kirschke, S., Bousquet, P., Ciais, P., Saunois, M., Canadell, J. G., Dlugokencky, E. J., Bergamaschi, P., Bergmann, D., Blake, D. R., Bruhwiler, L., Cameron-Smith, P., Castaldi, S., Chevallier, F., Feng, L., Fraser, A., Heimann, M., Hodson, E. L., Houweling, S., Josse, B., Fraser, P. J., Krummel, P. B., Lamarque, J.-F., Langenfelds, R. L., Le Quéré, C., Naik, V., O'Doherty, S., Palmer, P. I., Pison, I., Plummer, D., Poulter, B., Prinn, R. G., Rigby, M., Ringeval, B., Santini, M., Schmidt, M., Shindell, D. T., Simpson, I. J., Spahni, R., Steele, L. P., Strode, S. A., Sudo, K., Szopa, S., van der Werf, G. R., Voulgarakis, A., van Weele, M., Weiss, R. F., Williams, J. E., and Zeng, G.: Three decades of global methane sources and sinks, Nat. Geosci., 6, 813-823, 10.1038/ngeo1955, 2013.

Kobayashi, S., Ota, Y., Harada, Y., Ebita, A., Moriya, M., Onoda, H., Onogi, K., Kamahori, H., Kobayashi, C., Endo, H., Miyaoka, K., and Takahashi, K.: The JRA-55 Reanalysis: General Specifications and Basic Characteristics, J. Meteor. Soc. Japan, 93, 5-48, 10.2151/jmsj.2015-001, 2015.

Lehner, B., and Döll, P.: Development and validation of a global database of lakes, reservoirs and wetlands, Journal of Hydrology, 296, 1-22, https://doi.org/10.1016/j.jhydrol.2004.03.028, 2004.

Lin, J. C., Gerbig, C., Wofsy, S. C., Andrews, A. E., Daube, B. C., Davis, K. J., and Grainger, C. A.: A near-field tool for simulating the upstream influence of atmospheric observations: The Stochastic Time-Inverted Lagrangian Transport (STILT) model, J. Geophys. Res.-Atmos., 108, Doi 10.1029/2002jd003161, 2003.

Lin, J. C., Gerbig, C., Wofsy, S. C., Andrews, A. E., Daube, B. C., Grainger, C. A., Stephens, B. B., Bakwin, P. S., and Hollinger, D. Y.: Measuring fluxes of trace gases at regional scales by Lagrangian observations: Application to the CO_2 Budget and Rectification Airborne (COBRA) study, J. Geophys. Res., 109, doi:10.1029/2004JD004754, 2004.

Lin, J. C., and Gerbig, C.: Accounting for the effect of transport errors on tracer inversions, Geophys. Res. Lett., 32, 10.1029/2004GL021127, 2005.

McGuire, A. D., Anderson, L. G., Christensen, T. R., Dallimore, S., Guo, L., Hayes, D. J., Heimann, M., Lorenson, T. D., Macdonald, R. W., and Roulet, N.: Sensitivity of the carbon cycle in the Arctic to climate change, Ecol. Monogr., 79, 523-555, 10.1890/08-2025.1, 2009

Melton, J. R., Wania, R., Hodson, E. L., Poulter, B., Ringeval, B., Spahni, R., Bohn, T., Avis, C. A., Beerling, D. J., Chen, G., Eliseev, A. V., Denisov, S. N., Hopcroft, P. O., Lettenmaier, D. P., Riley, W. J., Singarayer, J. S., Subin, Z. M., Tian, H., Zürcher, S., Brovkin, V., van Bodegom, P. M., Kleinen, T., Yu, Z. C., and Kaplan, J. O.: Present state of global wetland extent and wetland methane modelling: conclusions from a model inter-comparison project (WETCHIMP), Biogeosciences, 10, 753-788, 10.5194/bg-10-753-2013, 2013.

Michalak, A. M., Bruhwiler, L., and Tans, P.: A geostatistical approach to surface flux estimation of atmospheric trace gases, J. Geophys. Res., 109, 10.1029/2003jd004422, 2004.

Miller, S. M., Worthy, D. E. J., Michalak, A. M., Wofsy, S. C., Kort, E. A., Havice, T. C., Andrews, A. E., Dlugokencky, E. J., Kaplan, J. O., Levi, P. J., Tian, H., and Zhang, B.: Observational constraints on the distribution, seasonality, and environmental predictors of North American boreal methane emissions, Global Biogeochem. Cycles, 28, 146-160, 10.1002/2013GB004580, 2014.

Nakazawa, T., Ishizawa, M., Higuchi, K., and Trivett, N. B. A.: Two curve fitting methods applied to CO_2 flask data, Environmtrics, 8, 197-218, 1997.

Olefeldt, D., Goswami, S., Grosse, G., Hayes, D., Hugelius, G., Kuhry, P., McGuire, A. D., Romanovsky, V. E., Sannel, A. B. K., Schuur, E. A. G., and Turetsky, M. R.: Circumpolar distribution and carbon storage of thermokarst landscapes, Nature Communications, 7, 13043, 10.1038/ncomms13043, 2016.

Patra, P. K., Houweling, S., Krol, M., Bousquet, P., Belikov, D., Bergmann, D., Bian, H., Cameron-Smith, P., Chipperfield, M. P., Corbin, K., Fortems-Cheiney, A., Fraser, A., Gloor, E., Hess, P., Ito, A., Kawa, S. R., Law, R. M., Loh, Z., Maksyutov, S., Meng, L., Palmer, P. I., Prinn, R. G., Rigby, M., Saito, R., and Wilson, C.: TransCom model simulations of CH_4 and related species: linking transport, surface flux and chemical loss with CH_4 variability in the troposphere and lower stratosphere, Atmos. Chem. Phys., 11, 12813-12837, 10.5194/acp-11-12813-2011, 2011.

Poulter , B., Bousquet, P., Canadell, J., G. , Philippe, C., Philippe, Peregon, A., Marielle, S., Arora, V., K., Beerling, D., J. , Victor, B., Chris, D. J., Fortunat, J., Nicola, G., Akihito, I., Thomas, K., Charles, D. K., Kyle, M., Joe, R. M., Changhui, P., Shushi, P., Catherine, P., Ronny, S., William, J. R., Makoto, S., Renato, S., Hanqin, T., Lyla,

T., Nicolas, V., David, W., Andy, W., Xiyan, X., Bowen, Z., Zhen, Z., and Qiuan, Z.: Global wetland contribution to 2000–2012 atmospheric methane growth rate dynamics, Environ. Res. Lett., 12, 094013, 2017.

Rodgers, C. D.: Inverse Methods for Atmospheric Sounding: Theory and Practice, World Scientific, 2000.

Saunois, M., Bousquet, P., Poulter, B., Peregon, A., Ciais, P., Canadell, J. G., Dlugokencky, E. J., Etiope, G., Bastviken, D., Houweling, S., Janssens-Maenhout, G., Tubiello, F. N., Castaldi, S., Jackson, R. B., Alexe, M., Arora, V. K., Beerling, D. J., Bergamaschi, P., Blake, D. R., Brailsford, G., Brovkin, V., Bruhwiler, L., Crevoisier, C., Crill, P., Covey, K., Curry, C., Frankenberg, C., Gedney, N., Höglund-Isaksson, L., Ishizawa, M., Ito, A., Joos, F., Kim, H. S., Kleinen, T., Krummel, P., Lamarque, J. F., Langenfelds, R., Locatelli, R., Machida, T., Maksyutov, S., McDonald, K. C., Marshall, J., Melton, J. R., Morino, I., Naik, V., O'Doherty, S., Parmentier, F. J. W., Patra, P. K., Peng, C., Peng, S., Peters, G. P., Pison, I., Prigent, C., Prinn, R., Ramonet, M., Riley, W. J., Saito, M., Santini, M., Schroeder, R., Simpson, I. J., Spahni, R., Steele, P., Takizawa, A., Thornton, B. F., Tian, H., Tohjima, Y., Viovy, N., Voulgarakis, A., van Weele, M., van der Werf, G. R., Weiss, R., Wiedinmyer, C., Wilton, D. J., Wiltshire, A., Worthy, D., Wunch, D., Xu, X., Yoshida, Y., Zhang, B., Zhang, Z., and Zhu, Q.: The global methane budget 2000–2012, Earth Syst. Sci. Data, 8, 697-751, 10.5194/essd-8-697-2016, 2016.

Schuur, E. A. G., McGuire, A. D., Schadel, C., Grosse, G., Harden, J. W., Hayes, D. J., Hugelius, G., Koven, C. D., Kuhry, P., Lawrence, D. M., Natali, S. M., Olefeldt, D., Romanovsky, V. E., Schaefer, K., Turetsky, M. R., Treat, C. C., and Vonk, J. E.: Climate change and the permafrost carbon feedback, Nature, 520, 171-179, 10.1038/nature14338, 2015.

Skamarock, W. C., Klemp, J. B., Dudhia, J., Gill, D. O., Baker, D. M., Huang, X.-Y., Wang, W., and Powers, J. G.: A Description of the Advanced Reserach WRF Version4, NCAR Technical Notes NCAR/TN-4751STR, 2008.

Stohl, A., Forster, C., Frank, A., Seibert, P., and Wotawa, G.: Technical note: The Lagrangian particle dispersion model FLEXPART version 6.2, Atmos. Chem. Phys., 5, 2461-2474, 10.5194/acp-5-2461-2005, 2005.

Stohl, A., Seibert, P., Arduini, J., Eckhardt, S., Fraser, P., Greally, B. R., Lunder, C., Maione, M., Mühle, J., O'Doherty, S., Prinn, R. G., Reimann, S., Saito, T., Schmidbauer, N., Simmonds, P. G., Vollmer, M. K., Weiss, R. F., and Yokouchi, Y.: An analytical inversion method for determining regional and global emissions of greenhouse gases: Sensitivity studies and application to halocarbons, Atmos. Chem. Phys., 9, 1597-1620, 10.5194/acp-9-1597-2009, 2009.

Tarantola, A.: Inverse Problem Theory: Methods for Data Fitting and Parameter Estimation, Elsevier Sci., New York, 1987.

Tarnocai, C., Canadell, J. G., Schuur, E. A. G., Kuhry, P., Mazhitova, G., and Zimov, S.: Soil organic carbon pools in the northern circumpolar permafrost region, Global Biogeochem. Cycles, 23, doi:10.1029/2008GB003327, 2009.

Thompson, R. L., Sasakawa, M., Machida, T., Aalto, T., Worthy, D., Lavric, J. V., Lund Myhre, C., and Stohl, A.: Methane fluxes in the high northern latitudes for 2005–2013 estimated using a Bayesian atmospheric inversion, Atmos. Chem. Phys., 17, 3553-3572, 10.5194/acp-17-3553-2017, 2017.

Thornton, B. F., Wik, M., and Crill, P. M.: Double-counting challenges the accuracy of high-latitude methane inventories, Geophys. Res. Lett., 43, 12,569-512,577, 10.1002/2016GL071772, 2016.

Uppala, S. M., KÅllberg, P. W., Simmons, A. J., Andrae, U., Bechtold, V. D. C., Fiorino, M., Gibson, J. K., Haseler, J., Hernandez, A., Kelly, G. A., Li, X., Onogi, K., Saarinen, S., Sokka, N., Allan, R. P., Andersson, E., Arpe, K., Balmaseda, M. A., Beljaars, A. C. M., Berg, L. V. D., Bidlot, J., Bormann, N., Caires, S., Chevallier, F., Dethof, A., Dragosavac, M., Fisher, M., Fuentes, M., Hagemann, S., Hólm, E., Hoskins, B. J., Isaksen, L., Janssen, P. A. E. M., Jenne, R., Mcnally, A. P., Mahfouf, J. F., Morcrette, J. J., Rayner, N. A., Saunders, R. W., Simon, P., Sterl, A., Trenberth, K. E., Untch, A., Vasiljevic, D., Viterbo, P., and Woollen, J.: The ERA-40 re-analysis, Q. J. R. Meteorolog. Soc., 131, 2961-3012, doi:10.1256/qj.04.176, 2005.

Worthy, D. E. J., Chan, E., Ishizawa, M., Chan, D., Poss, C., Dlugokencky, E. J., Maksyutov, S., and Levin, I.: Decreasing anthropogenic methane emissions in Europe and Siberia inferred from continuous carbon dioxide and methane observations at Alert, Canada, J. Geophys. Res., 114, 10.1029/2008JD011239, 2009.

Zhao, C., Andrews, A. E., Bianco, L., Eluszkiewicz, J., Hirsch, A., MacDonald, C., Nehrkorn, T., and Fischer, M. L.: Atmospheric inverse estimates of methane emissions from Central California, J. Geophys. Res., 114, D16302, 10.1029/2008JD011671, 2009.

Table 1. ECCC atmospheric measurements sites in the Canadian Arctic.

Site	ID	Latitude [˚]	Longitude [˚]	Elevation [m]	Sampling height [m]	Start (conti.) Start (flask)
Alert	ALT	82.5N	62.5W	200	10	1988/01 1999/10
Behchoko[a]	BCK	62.8N	115.9W	160	60	2010/10 NA
Inuvik[a]	INU	68.3N	133.5W	113	10	2012/02 2012/05
Cambridge Bay[a]	CBY	69.1N	105.1W	35	10	2012/12 2012/12
Baker Lake	BKL	64.3N	96.0W	95	10	2014/06 2017/07
Churchill[a]	CHL	58.7N	93.8W	29	60	2007/05 2011/10

[a] The sites are used in the inversion in this study

Table 2. Three cases of prior emissions.

Source	VIS	GEL	WetC
Wetland[1]	VISIT	VISIT (optimized, as Natural[1])	WetCHARTs Extended (Ver.1.0)
Soil Uptake[2]	VISIT	VISIT (optimized, as Soil Uptake[2])	VISIT (optimized, as Soil Uptake[2])
Anthropogenic[3] (excl. Rice cultivation)	EDGARv4.2FT2010	EDGARv4.2FT2010 (optimized as Anthropogenic[3])	EDGARv4.2FT2010 (optimized as Anthropogenic[3])
Biomass Bunning[4]	GFASv1.2	GFASv1.2	GFASv1.2
Rice cultivation[1]	VISIT	VISIT (optimized, as Natural[1])	VISIT (optimized, as Natural[1])
Termites[1]	GISS	GISS (optimized, as Natural[1])	GISS (optimized, as Natural[1])

~~C1~~ VIS used the same prior fluxes with those for global GELCA-CH_4 inversion except Biomass Burning. GELCA-CH_4 inversion optimised CH_4 fluxes for 4 source types, 1) natural, 2) soil uptake, 3) anthropogenic and 4) biomass burning, which are also indicated by superscripted numbers. ~~C2~~ GEL used the posterior fluxes from global GELCA-CH_4 inversion. For ~~C1~~ VIS and ~~C2~~ GEL, five-year mean of each source type was used. ~~C3~~ WetC used WetCHARTs extended mean fluxes as wetland CH_4, while other fluxes were same with ~~C3~~ GEL. For all the scenarios, GFAS v1.2 daily fluxes are used as biomass burning.

Table 3. Experiment configurations. Using each of 3 different masks (A, B and C in Fig. S3), 9 inversion runs were conducted with a combination of 3 prior emission cases (~~C1, C2,C3~~ VIS, GEL and WetC on Table 2) and 3 different models (FLEXPART_EI, FLEXPART_JRA55 and WRF-STILT). Totally 27 inversion runs were conducted.

Exp	Mask					
	Mask A (NT, YT, NU)		Mask B (NT+NT, NU)		Mask C (NT+NT+NU)	
	Fluxes	Model	Fluxes	Model	Fluxes	Model
Exp1	VIS	FLEXPART_EI	VIS	FLEXPART_EI	VIS	FLEXPART_EI
Exp2	VIS	FLEXPART_JRA55	VIS	FLEXPART_JRA55	VIS	FLEXPART_JRA55
Exp3	VIS	WRF-STILT	VIS	WRF-STILT	VIS	WRF-STILT
Exp4	GEL	FLEXPART_EI	GEL	FLEXPART_EI	GEL	FLEXPART_EI
Exp5	GEL	FLEXPART_JRA55	GEL	FLEXPART_JRA55	GEL	FLEXPART_JRA55
Exp6	GEL	WRF-STILT	GEL	WRF-STILT	GEL	WRF-STILT
Exp7	WetC	FLEXPART_EI	WetC	FLEXPART_EI	WetC	FLEXPART_EI
Exp8	WetC	FLEXPART_JRA55	WetC	FLEXPART_JRA55	WetC	FLEXPART_JRA55
Exp9	WetC	WRF-STILT	WetC	WRF-STILT	WetC	WRF-STILT

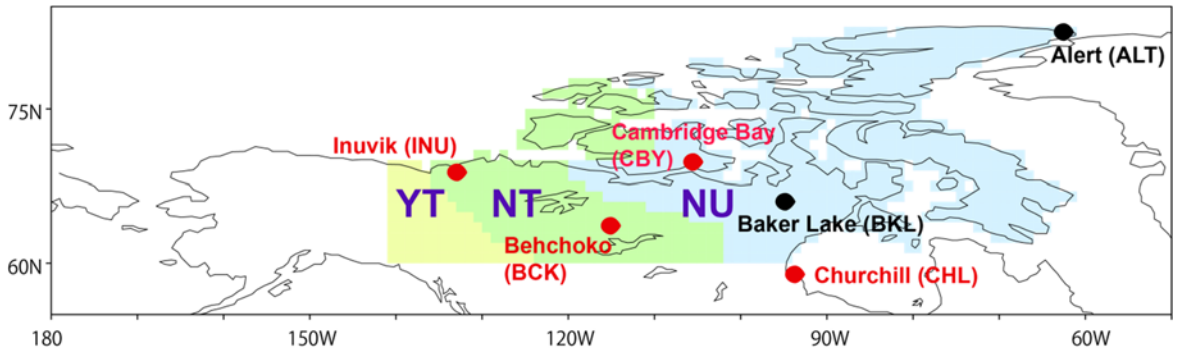

Figure 1: The ECCC atmospheric measurement sites around the Arctic. The sites used for the inversion are indicated in red. The three shaded areas are the three territories which are used as sub-regions in the inversions: YT (Yukon), NT (Northwest Territories) and NU (Nunavut).

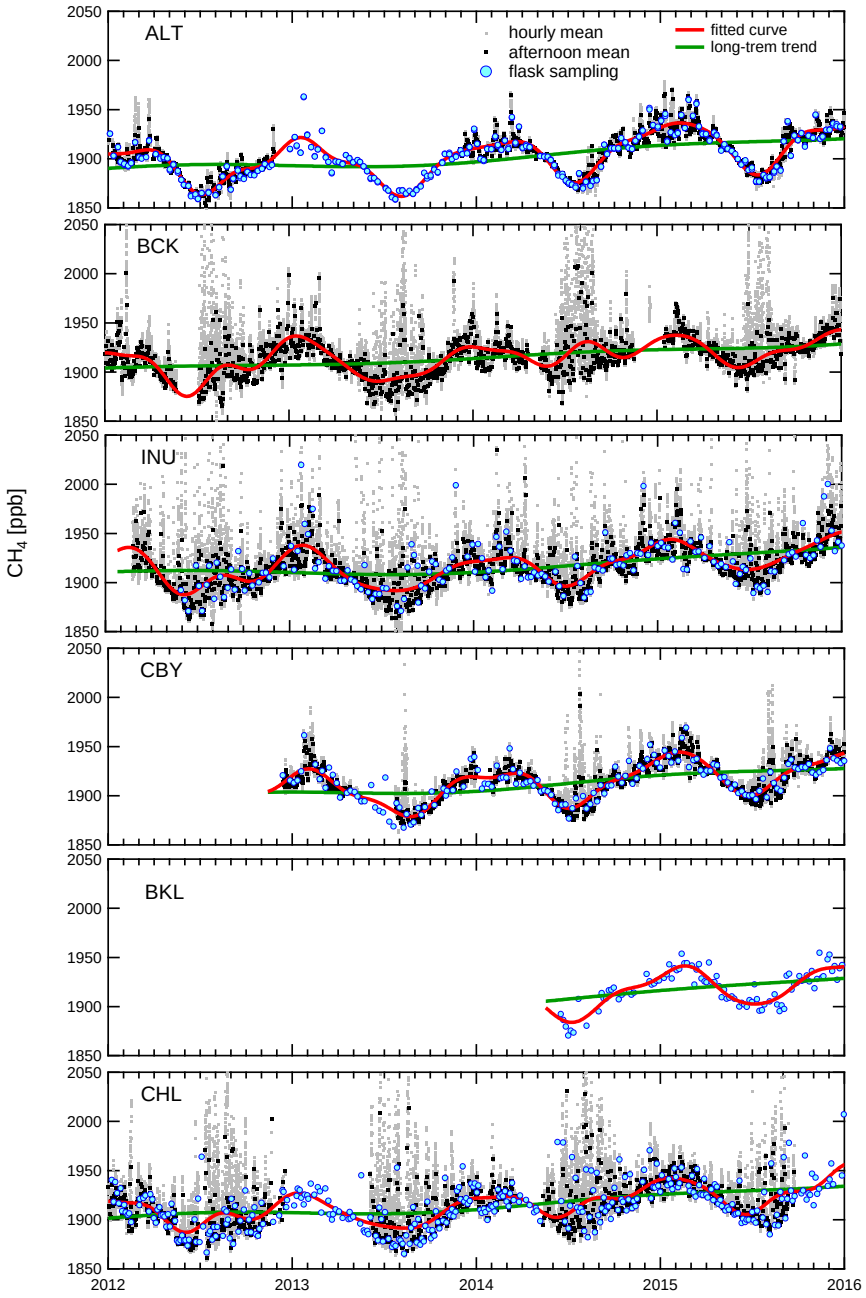

Figure 2: Time-series of atmospheric CH_4 ~~concentrations~~ mixing ratios at Canadian Arctic sites. The observed values are the hourly means (grey dot), the afternoon means (black dot, 12:00─16:00 local time) from the continuous measurements and the ones from flask sampling (circle in light blue). BCK has only continuous measurements. At BKL, flask air sampling is only available after being initiated in 2014. The red and green curves are fitted curves and long-term trends which are obtained by applying a fitting-curve method to the observed afternoon means.

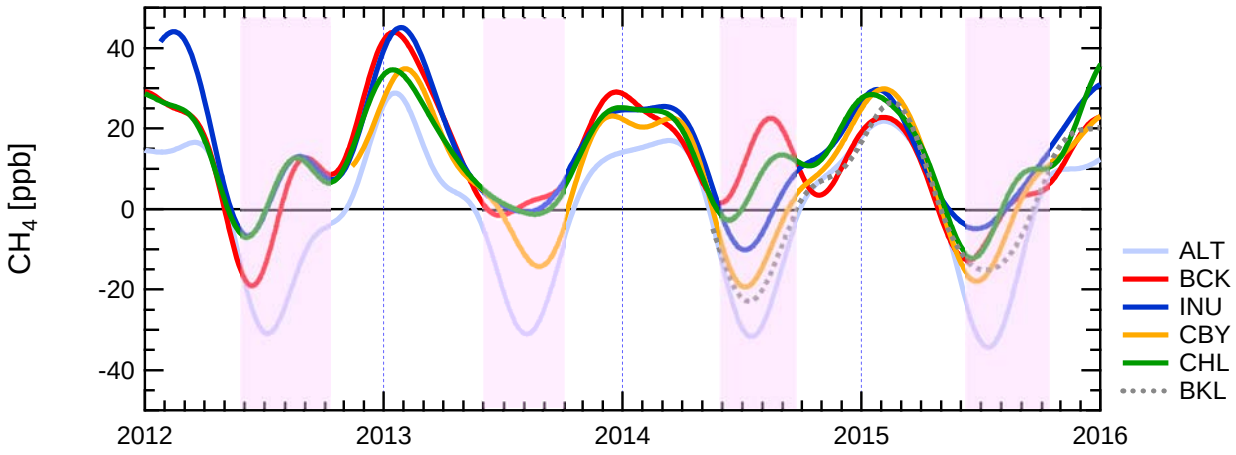

Figure 3: Seasonal components in fitted curves of observed atmospheric CH_4 ~~concentrations~~ mixing ratios at Canadian Arctic Sites. Each fitted curve has subtracted the long-term trend component of Alert. Summer months (June—September) are highlighted by light pink shaded background.

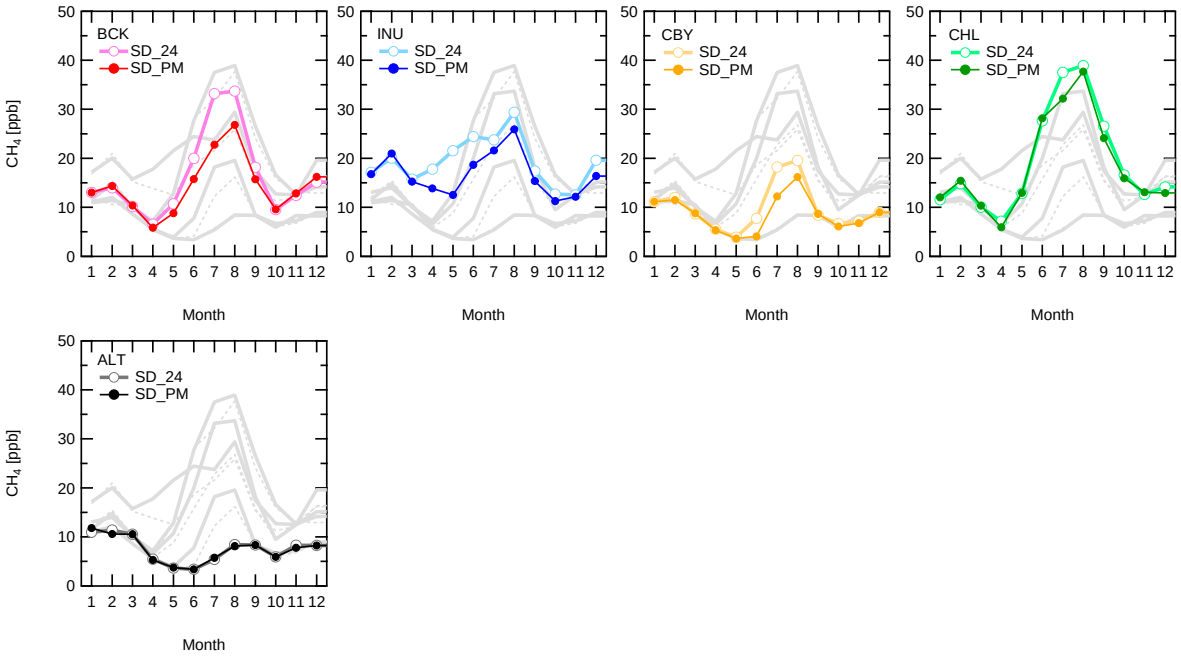

Figure 4: Mean seasonal cycles of monthly standard deviation (SD) of observed CH_4 ~~concentrations~~ mixing ratios, SD_24 of all 24 hourly data (closed circles) and SD_PM of afternoon data (12:00─16:00 local time, open circles) to the fitted curves respectively. For BCK, 2014 data have been excluded from the analysis, because of high variability due to massive large forest fires around the site.

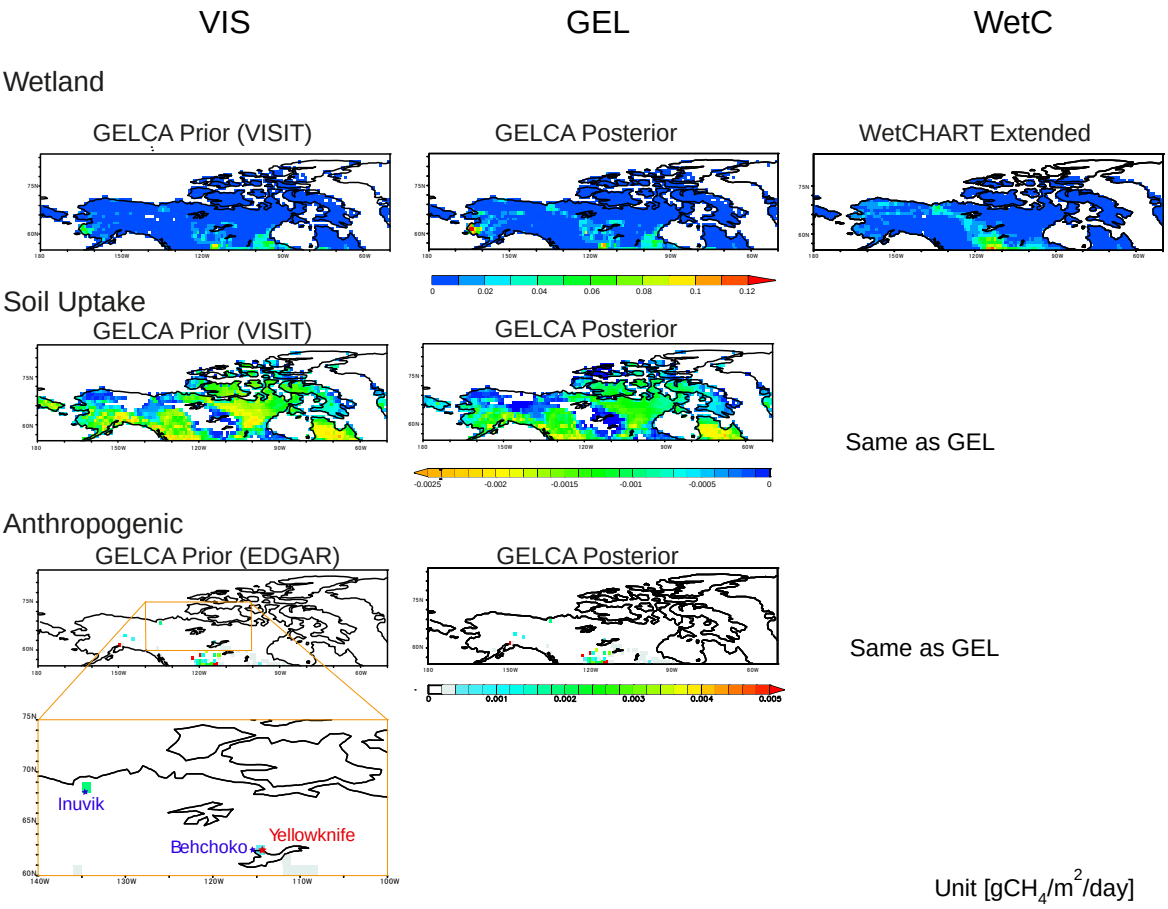

Figure 5: Spatial distributions of summertime prior CH_4 fluxes of wetland emission, soil uptake and anthropogenic emissions for the three cases of prior fluxes, ~~C1, C2, and C3~~ VIS, GEL and WetC, which are listed in table 2. Bottom left panel is a zoomed anthropogenic emission distribution in Northwest Territories. The locations of two sites, Behchoko (BCK) and Inuvik (INU) and the capital city, Yellowknife, are also plotted.

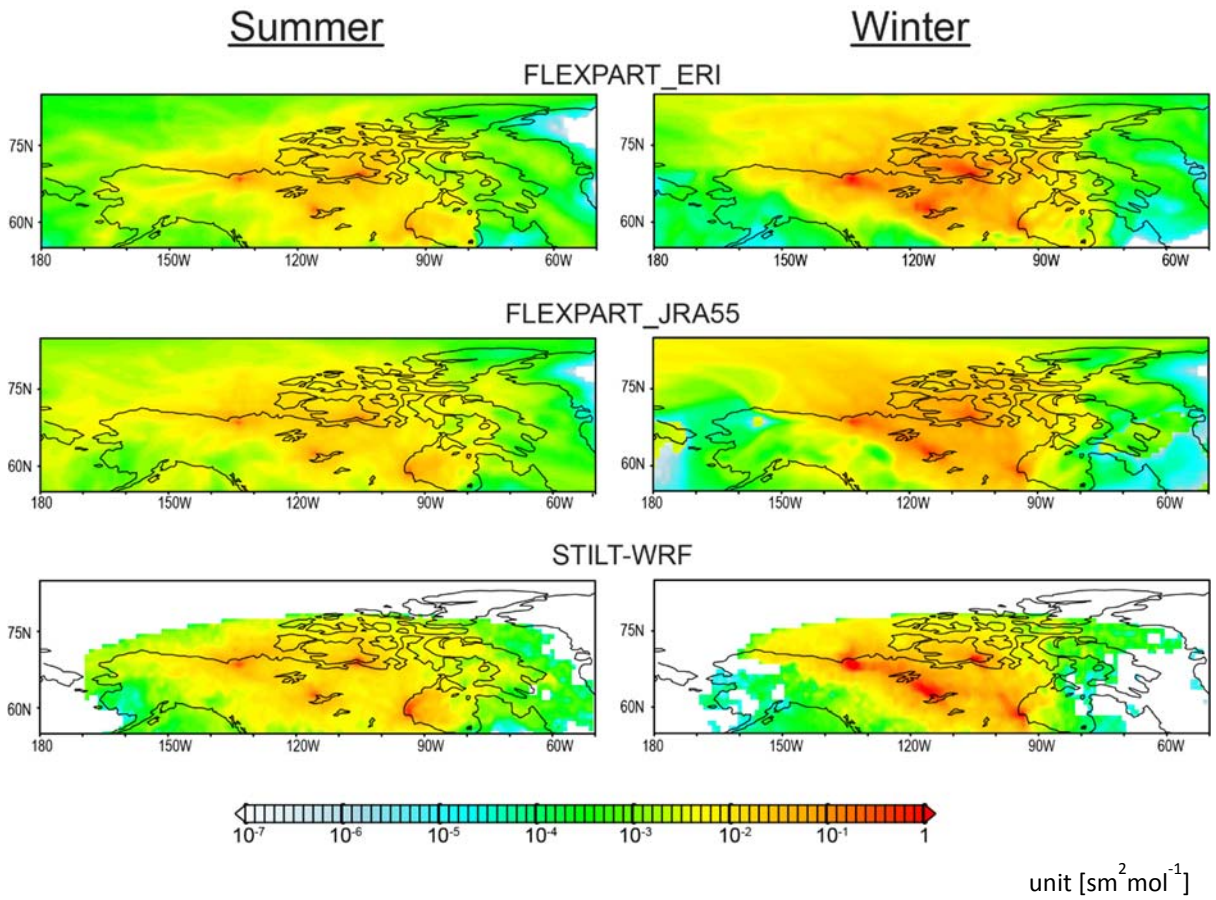

5

Figure 6: Seasonal mean footprints of all sites by three models, shown for summer, July─August 2013) and winter (January─February 2013).

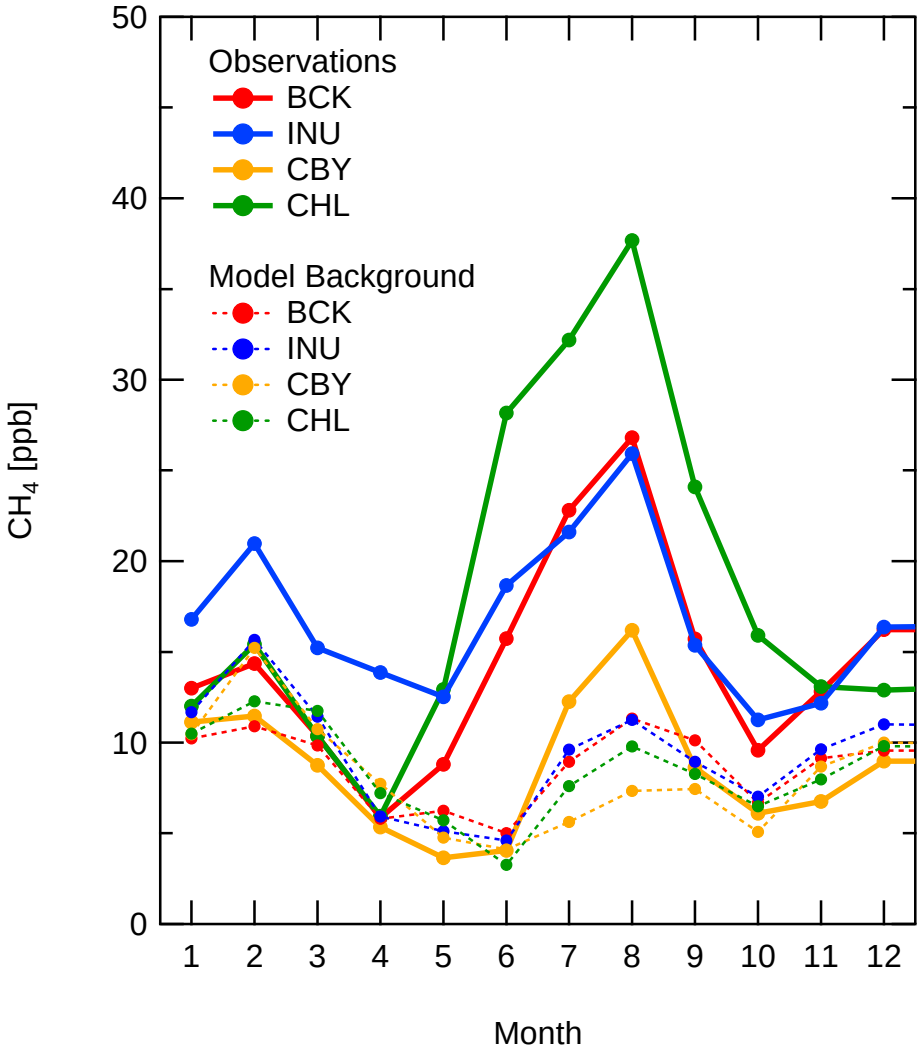

Figure 7: Four-year (2012–2015) mean monthly SD of modelled background CH_4 ~~concentrations~~ mixing ratios and SD of observed CH4 ~~concentrations~~ mixing ratios (afternoon data only, SD_PM). The background CH_4 ~~concentrations~~ mixing ratios are NIES-TM modelled ~~concentrations~~ mixing ratios weighted by the endpoints of 5-day back trajectory.

5

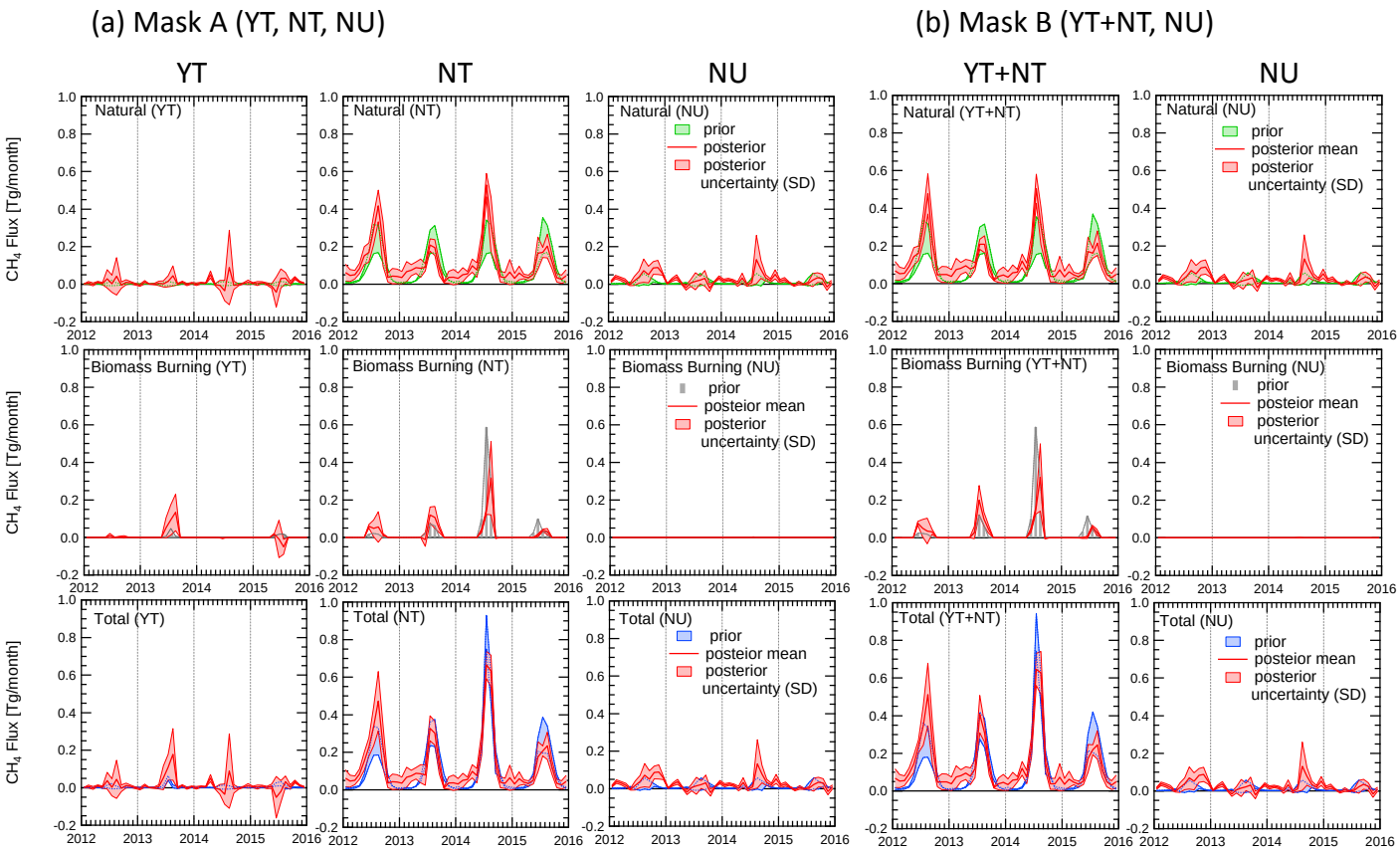

Figure 8: Monthly posterior mean fluxes with (a) sub-region Mask A (YT, NT, NU) and (b) Mask B (YT+NT, NU). Posterior mean flux is an average of nine experiments with 3 models (FLEXPART_EI, FLEXPART_JRA55 and WRF-STILT) and 3 prior emission cases (~~C1, C2, and C3~~ VIS, GEL and WetC). The posterior SD is shown by the red shaded area. Prior fluxes for natural include wetland flux, soil uptake and anthropogenic emissions. Biomass burning prior fluxes are from GFAS. The (non-red) shaded areas for natural and total prior fluxes indicate the range of prior fluxes.

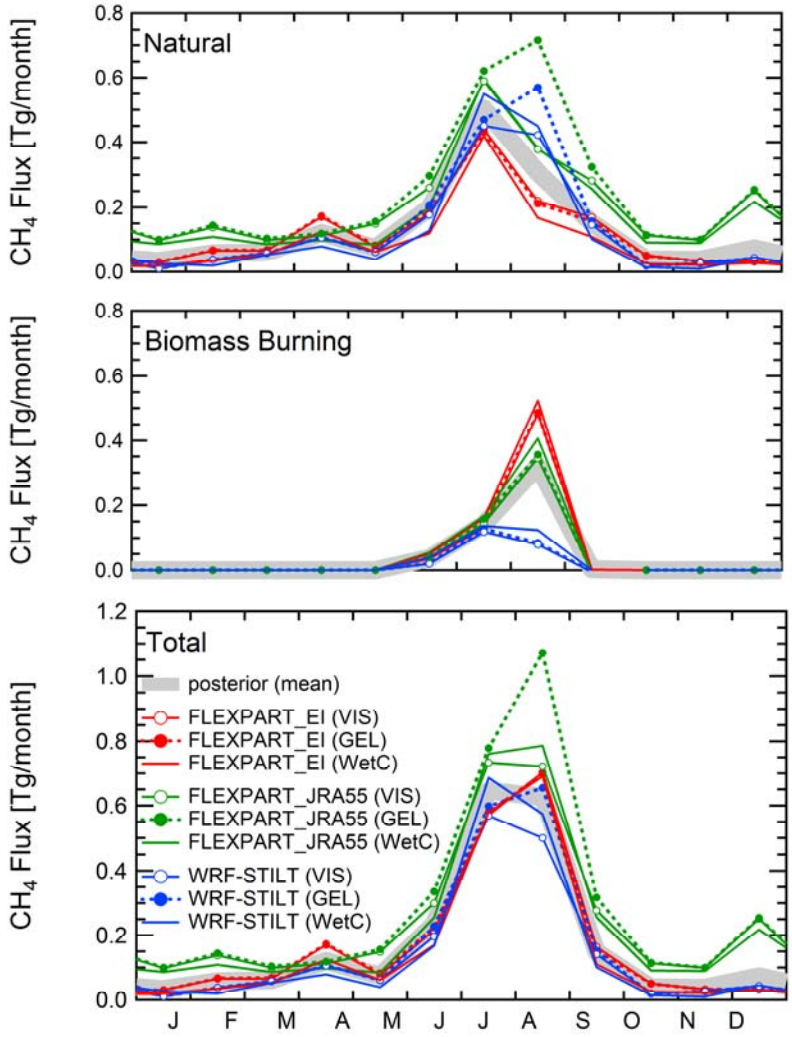

Figure 9: Examples of monthly posterior fluxes by 9 inversion experiments of 3 different models (FLEXPART_EI, FLEXPART_JRA55 and WRF-STILT) with 3 prior emission cases (~~C1, C2, and C3~~ VIS, GEL and WetC). The posterior fluxes are plotted for sub-region YT+NT in Mask B. The posterior flux means over all nine experiments with Mask B are also plotted.

(a) Mean annual Fluxes

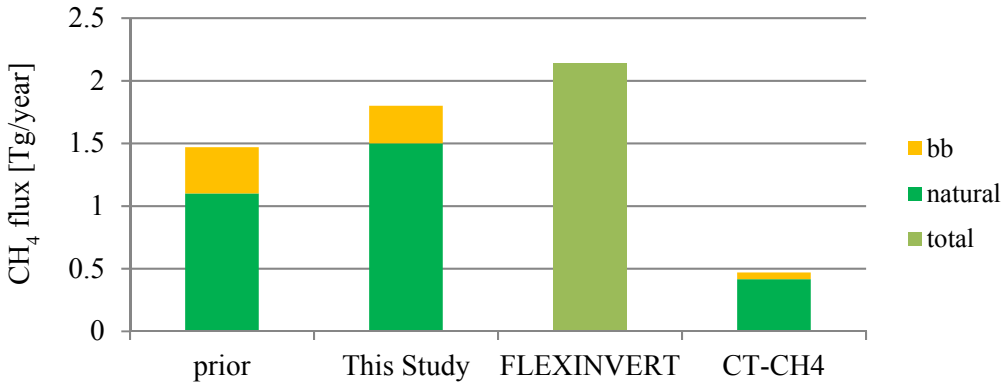

(b) Mean monthly Fluxes

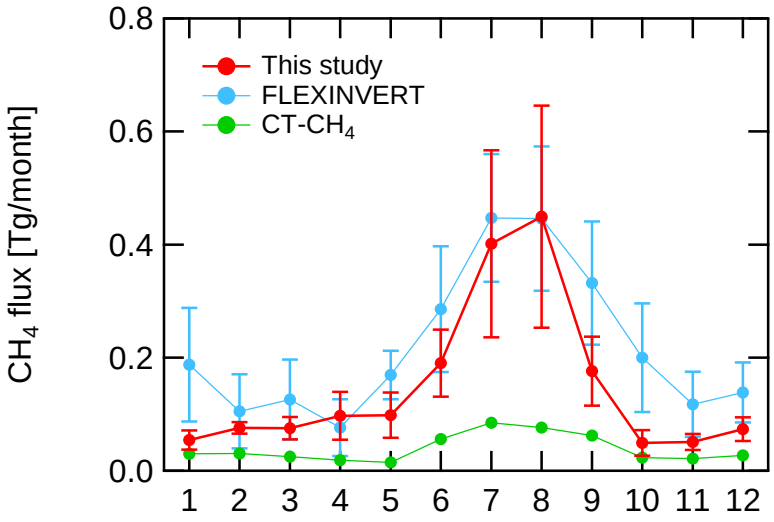

Figure 10: mean prior and posterior (a) annual and (b) monthly fluxes for the Canadian Arctic. FLEXINVERT (Thompson et al., 2017) and CarbonTracker-CH_4 (CT-CH_4, Bruhwiler et al. (2014)) are plotted for comparison. FLEXINVERT and CT-CH_4 fluxes are their last 5-year means, that is, 2009–2013 and 2006–2010 respectively. "natural" in CT-CH_4 are combined with the fluxes estimated as "anthropogenic" and "agriculture". The bars in monthly fluxes are SD of multi-year mean monthly fluxes.

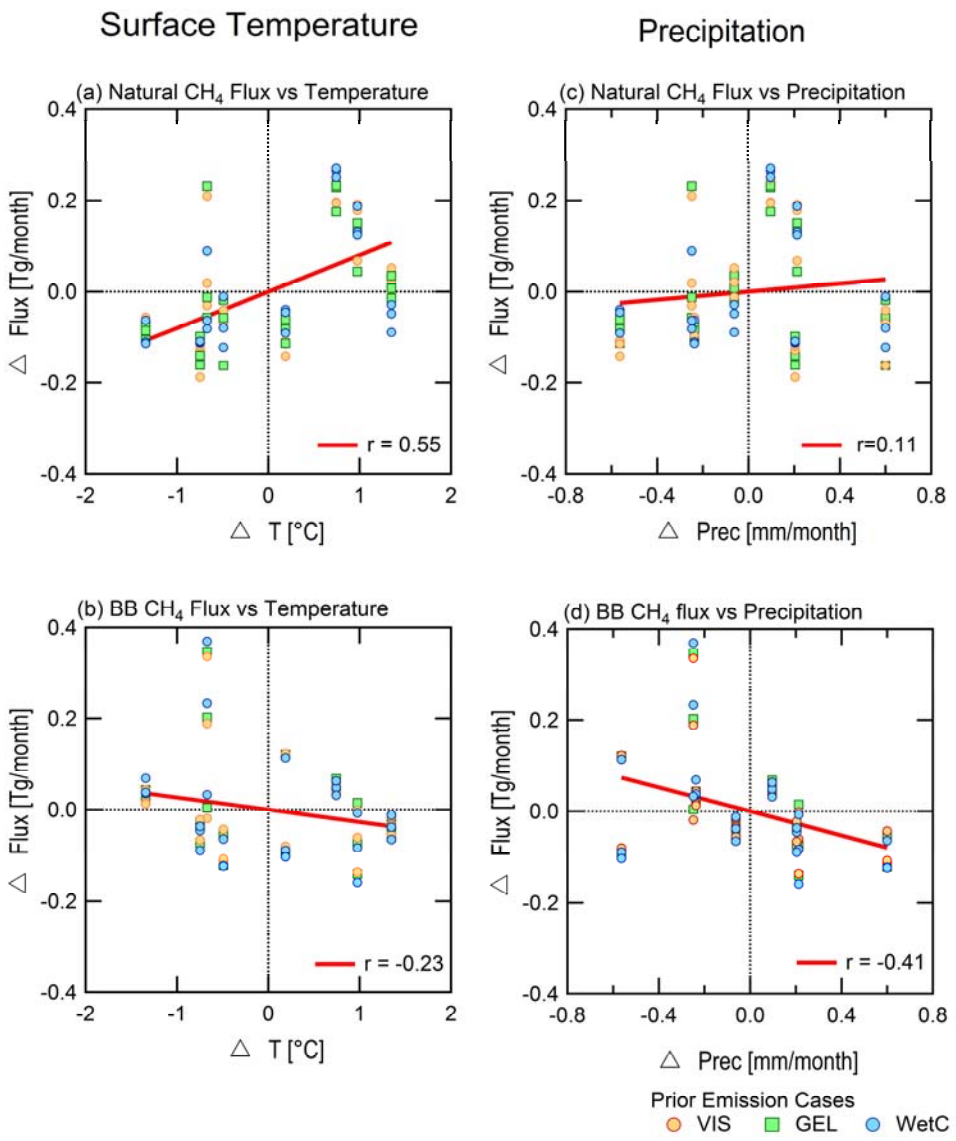

Figure ~~12~~ 11: CH_4 flux anomalies vs surface temperature and precipitation anomalies for summer (July and August). The CH_4 fluxes are July and August posterior fluxes for ~~the Canadian Arctic~~ Northwest Territories (NT) from 9 inversion experiments with Mask ~~C~~ A. Regional climate parameter anomalies in NT are monthly deviations from the four-year (2012–2015) means

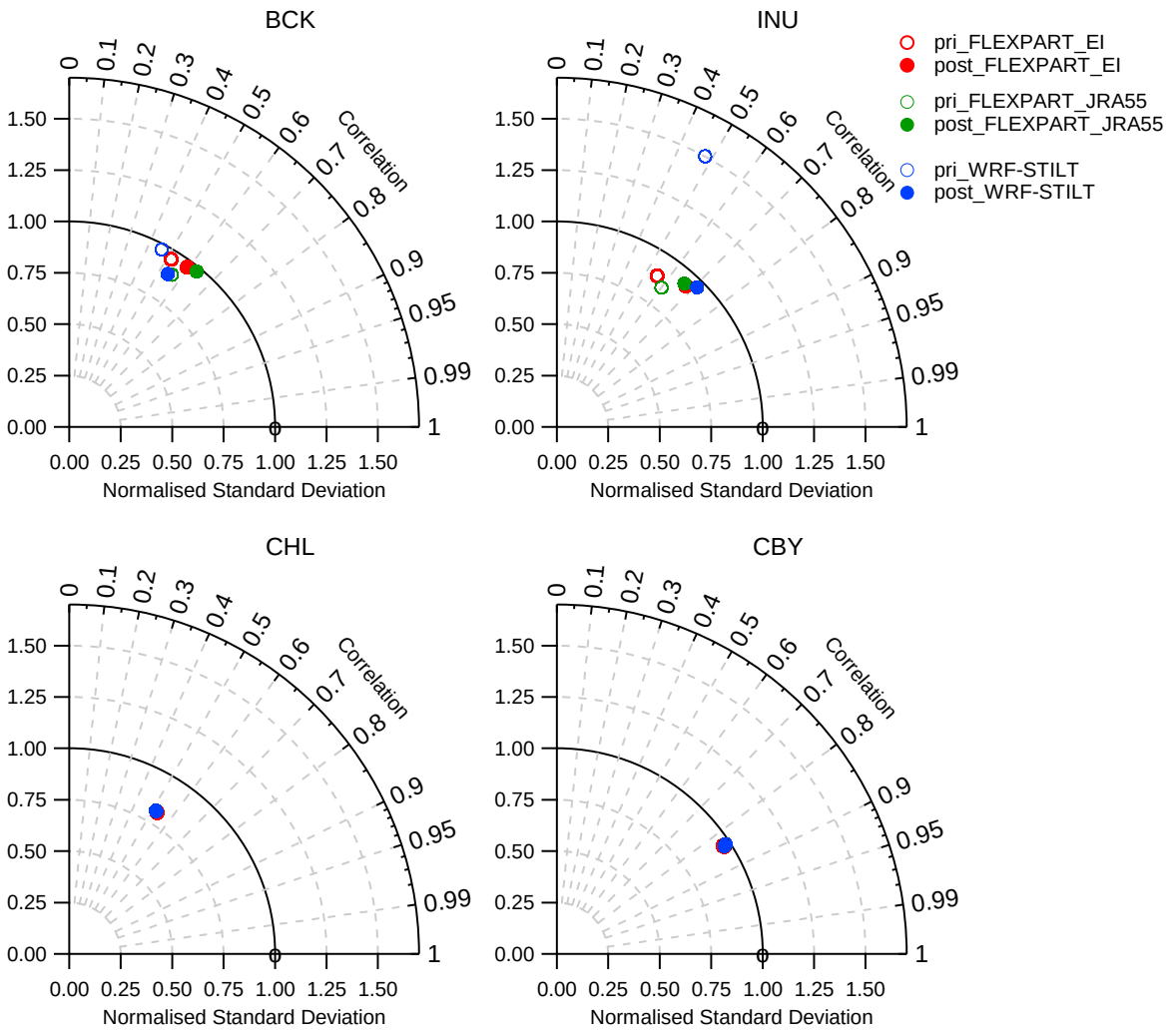

Figure ~~11~~ 12: Taylor diagrams for the comparison between the prior (open circles) and posterior (closed circles) ~~concentrations~~ mixing ratios by three models: FLEXPART_EI (red), FLEXPART_JRA55 (green), and WRF-STILT (blue), with Mask B and prior flux case ~~C3~~ WetC. The radius is the normalised standard deviation (NSD) of modelled ~~concentrations~~ mixing ratios against observations. The angle is the correlation coefficient. The values are the means with all observations and modelled ~~concentration~~ mixing ratios per each simulation for each site.